Mon. Not. R. Astron. Soc. **389,** 1577–1592 (2008) doi:10.1111/j.1365-2966.2008.13694.x

Light-curve studies of nearby Type Ia supernovae with a Multiband Stretch method

N. Takanashi,[1,2]★ M. Doi[1] and N. Yasuda[3]

[1]*Institute of Astronomy, Graduate School of Science, University of Tokyo, 2-21-1 Osawa, Mitaka, Tokyo 181-0015, Japan*
[2]*National Astronomical Observatory of Japan, Mitaka 181-8588, Japan*
[3]*Institute for Cosmic Ray Research, University of Tokyo, Kashiwa 277-8582, Japan*

Accepted 2008 July 7. Received 2008 July 7; in original form 2007 November 2

ABSTRACT

We create new *U*-, *B*-, *V*-, *R*- and *I*-band light-curve templates of Type Ia supernovae (SNe Ia) and re-analyse 122 nearby (redshift < 0.11) SNe Ia using a new 'Multiband Stretch method', which is a revised Stretch method extended to five bands. We find (i) our *I*-band template can fit about 90 per cent of SNe Ia *I*-band light curves, (ii) relationships between luminosity, colours and stretch factors, (iii) possible subgroups of SNe Ia and (iv) the ratio of total to selective extinction *R* in other galaxies can be consistent with that in the Milky Way under the assumption that SNe Ia have diversity in their intrinsic colour. Based on these results, we discuss how to select subsets of SNe Ia to serve as good distance indicators for cosmology. We find two possibilities: one is to choose 'BV bluest' $[-0.14 < (B - V)_{\max} \leq -0.10]$ objects and the other is to use only SNe Ia which occur in E or S0 galaxies. Within these subsets, we find the root mean square (rms) of peak *B*-band magnitudes is 0.17 mag ('BV bluest' sample) and 0.12 mag (E or S0 sample).

Key words: supernovae: general – distance scale.

1 INTRODUCTION

Type Ia supernovae (SNe Ia) are some of the most important objects in observational cosmology because of their role as distance indicators. SNe Ia are bright enough to be observed at high redshifts, they have uniform peak luminosity (cf. Branch et al. 1992), and are expected to evolve less from low to high z than other objects such as galaxies (cf. Riess et al. 1999b). Many studies have used SN Ia as distance indicators to show the accelerating expansion of the Universe (e.g. Riess et al. 1998; Perlmutter et al. 1999; Knop et al. 2003; Riess et al. 2004; Astier et al. 2006; Wood-Vasey et al. 2007). All of these works are based on the empirical relationship between light-curve shapes and peak luminosity (cf. Phillips 1993). From the 1990s onward, as more low-redshift SNe Ia have been found, the relation has been revised (cf. Hamuy et al. 1996a; Riess et al. 1999a; Altavilla et al. 2004; Reindl et al. 2005).

Recently, the number of well-measured SNe Ia has grown larger and larger, especially at intermediate and high redshifts. There are many SN survey programmes currently running; for example, the Lick Observatory and Tenagra Observatory Supernova Searches (LOTOSS[1]), the Nearby Supernova Factory (SNfactory, Aldering et al. 2002), the Sloan Digital Sky Survey-II Supernova Survey (SDSS-II SN Survey, Frieman et al. 2008; Sako et al. 2008), Equation of State: SupErNovae trace Cosmic Expansion (ESSENCE, Wood-Vasey et al. 2007), and the SuperNova Legacy Survey (SNLS, Pritchet et al. 2005). Most of the SNe Ia found in these surveys are observed in multiple passbands and over many epochs. These high-quality samples have given us clues to understand the nature of SNe Ia. For example, Hamuy et al. (1996b) showed that brighter SNe Ia, like SN1991T, tend to occur in galaxies with active star formation, while fainter SNe Ia, such as SN1991bg, tend to occur in galaxies which lack star formation (see also Howell 2001; van den Bergh, Li & Filippenko 2005; Sullivan et al. 2006). Benetti et al. (2005) discussed the intrinsic diversity of the spectroscopically normal SNe Ia (called 'Branch normal', Branch, Fisher & Nugent 1993). Quimby, Hoflich & Wheeler (2007) pointed out that there are two subgroups within Branch normal SNe Ia. Unusual SNe Ia have also been found: SN2000cx and SN2002cx were reported as an extreme sample of spectroscopically peculiar SNe Ia (Li et al. 2001, 2003). Howell et al. (2006) reported SNLS-03D3bb was a super-Chandrasekhar-mass SN with an exceptionally high luminosity and low kinetic energy. Hα emission in the spectra of SN2002ic and SN2005gj at early phases indicates the existence of circumstellar material around the progenitor (Deng, Kawabata & Ohyama 2004; Aldering et al. 2006 and so on).

Although SNe Ia seem to be good standard candles for cosmological studies, there are several issues we must understand in order to use them optimally. The main issues are (i) intrinsic photometric and spectroscopic diversity of SNe Ia and (ii) extinction in host galaxies. Both issues severely limit the use of SNe Ia as a standard candles if

★E-mail: naohiro.takanashi@nao.ac.jp
[1]http://astro.berkeley.edu/∼bait/lotoss.html

we cannot deal with them properly. Recent studies have revealed an intrinsic diversity of SNe Ia; for example, Mannucci et al. (2005) and Sullivan et al. (2006) showed that there are two types of SN Ia, called 'prompt' and 'delayed', which differ in the distribution of their stretch factors, and Berian et al. (2006) demonstrated how spectroscopic diversity can affect significantly the intrinsic colours of SNe Ia and *K*-corrections. The latter issue is important if we want to use larger SN Ia samples. Correction of extinction by dust in the host galaxy is necessary because almost all SNe Ia may be affected by the dust. Previous works insisted that the ratio of total to selective extinction, R_B, in other galaxies is smaller than that of the Milky Way; see Altavilla et al. (2004) (hereafter ALT04), Phillips et al. (1999) and Knop et al. (2003).

In this paper, we discuss these issues using a sample of nearby SNe Ia. We re-analyse published data on nearby SNe Ia with an improved 'Multiband Stretch method' which is based on the usual 'Stretch method' (Perlmutter et al. 1997; Goldhaber et al. 2001).

2 PHOTOMETRIC DATA

We use *U*-, *B*-, *V*-, *R*- and *I*-band light curves in the Vega system of 122 SNe in this work. All of the sample have *B*- and *V*-band photometry, but they do not always have *U*-, *R*- and *I*-band photometry (see Table 1). All photometric data are obtained from published papers, mainly from Jha et al. (2006) (hereafter JHA06), Riess et al. (1999a) and Hamuy et al. (1996a). We also took photometric data from Ford et al. (1993), Wells et al. (1994), Richmond et al. (1995), Patat, Benetti & Cappellaro (1996), Lira et al. (1998), Suntzeff et al. (1999), Krisciunas et al. (2000), Ho et al. (2001), Krisciunas et al. (2001), Modjaz, Li & Filippenko (2001), Strolger et al. (2002), Krisciunas et al. (2003), Li et al. (2003), Valentini et al. (2003), Vinko et al. (2003), Garnavich et al. (2004), Germany et al. (2004), Krisciunas et al. (2004a,b), Pignata et al. (2004), Anupama et al. (2005), Kuntal, Atish & Bhattacharya (2005) and Sahu, Anupama & Prabhu (2006). All of the SNe Ia used in this paper have *B*- and *V*-band data. We analysed only bands in which there are more than three measurements. For example, if a SN had five *B*-, five *V*- and two *I*-band measurements, we did not include its *I*-band photometry in our analysis. There are some SNe Ia which were observed by different groups independently, but we did not combine these light curves to avoid systematic errors; instead, we used the light curve with the largest number of epochs. Many of our data are also found in the compilations of ALT04 and Reindl et al. (2005). Fig. 1 shows the redshift distribution of our sample.

According to Reindl et al. (2005), there are five 'SN1991T-like' SNe (SN1991T, SN1995ac, SN1995bd, SN1997br and SN2000cx) and seven 'SN1991bg-like' SNe (SN1991bg, SN1992K, SN1997cn, SN1998bp, SN1998de, SN1999by and SN1999da) in our sample. The other 111 SNe either are 'Branch normal' or lack detailed spectroscopic analysis.

Table 1. Number of SNe Ia in each band.

Sample	*U* band	*B* band	*V* band	*R* band	*I* band
1A	49	122	122	101	115
1B	44	108	108	88	102

1A are all SNe Ia we analysed in this paper.
1B are selected SNe Ia based on χ^2 (see Section 3.2).

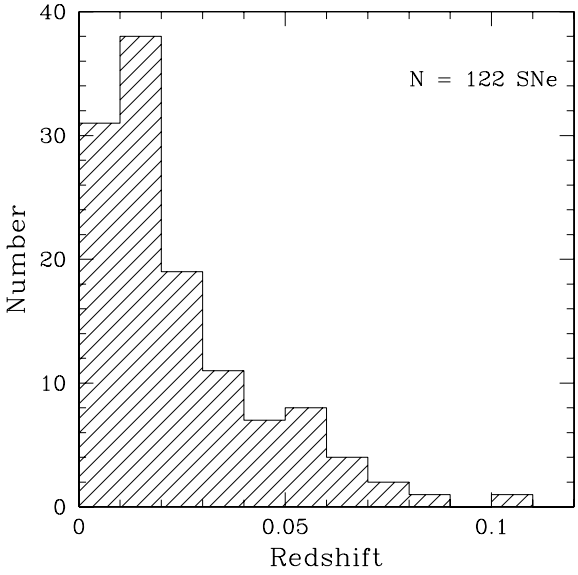

Figure 1. Redshift distribution of SNe Ia used in this work. Most of them are at $z < 0.02$.

3 ANALYSIS

3.1 Light-curve parametrization

There are several ways to describe the shape of a SN's light curve, but we can classify them roughly into two types. One type concentrates on the data in a single passband, such as the 'Δm_{15}' (Phillips 1993) or 'Stretch' (Perlmutter et al. 1997) algorithms. The other type includes measurements of light curves in multiple passbands, such as the 'multi-colour light-curve shape' (MLCS, MLCS2k2) method (Riess et al. 1996; Jha, Riess & Kirshner 2007), the 'colour–magnitude intercept calibration' (CMAGIC) (Wang, Goldhaber & Aldering 2003), and the 'spectral adaptive light curve template' (SALT, SALT2) (Guy et al. 2005, 2007) algorithms. The latter type is more complex and employs SN colours as a part of the analysis. Prieto, Armin & Suntzeff (2006) proposed a new method, a combination of Δm_{15} and MLCS, to gain the advantages from both approaches.

For this work, we chose the single-band Stretch method as a base, since it is simple to parametrize light curves: we just need one template for each band. We created new *U*-, *B*-, *V*-, *R*- and *I*-band templates (see Section 3.4), which we simply stretch to fit observed light curves, without having to account for additional assumptions such as dust extinction. This method works well when we simply want to assign a light-curve shape and peak apparent brightness in each band.

Usually, the Stretch method has been applied only to *B*- or *V*-band light curves. However, in this work, we apply the Stretch method to data in all passsbands: *U*, *B*, *V*, *R* and *I* band. In other words, we fit up to 11 parameters to each event: *U*-, *B*-, *V*-, *R*- and *I*-band stretch factors, *U*-, *B*-, *V*-, *R*- and *I*-band peak magnitudes, and a time $t_{B\max}$ for maximum light in the *B* band. The reason that we apply a stretch factor to *U*, *B*, *V*, *R* and *I* bands independently instead of a common stretch factor like SALT (Guy et al. 2005) is that we wish to investigate the diversity of light-curve shapes between passbands. We call this method the 'Multiband Stretch method'.

It is well known that there are some peculiarities in redder band light-curve shapes, especially in the *I* band. There are usually two peaks in *I*-band light curves, but some SNe Ia lack the second peak.

There are very few of these SNe Ia without the second peak in our sample, so we use only 'normal' *I*-band template for our analysis (see Section 4.3).

Using information in multiple passbands improves the determination of the time of *B*-band maximum brightness. By using data from the second peak in *R* and *I* band around 30–40 d after *B*-band maximum, we can determine the time of *B*-band maximum even if there are no observations around the first peak. In addition, as a result of fitting, we can use colour information to study the intrinsic colours of SNe Ia, the effects of dust extinction and so on.

Please note that we use the inverse of the usual stretch factor $(1/s)$ for easier comparison with the Δm_{15} parameter.

3.2 Fitting algorithm

We used a reduced χ^2 method for fitting templates to observations. Our definition of reduced χ^2 is as follows;

$$\chi^2 = \frac{1}{\text{d.o.f.}} \times \sum_X \sum_{i=0}^{n} \left(\frac{\Delta m}{\sqrt{\sigma_{\text{obs}}^2 + \sigma_{\text{temp}}^2}} \right)^2 \quad (1)$$

$$\{\Delta m = m_{Xi} - K_{X,(t_i - t_{B\max})/(1+z)} - M_X^{\text{temp}}[(1+z) \times (1/s_{(X)}) \times (t_i - t_{B\max})] - X_{\max} - \mu\}.$$

Here, n is the total number of observed epochs, d.o.f. is the number of degrees of freedom in the fitting, m_{Xi} is the observed apparent magnitude in the X band after correction for Galactic dust extinction from Schlegel, Finkbeiner & Davis (1998), $t_{B\max}$ is time of the maximum in the B band, $K_{X,t}$ is the K-correction in the X-band[2] magnitude at time $t - t_{B\max}$, μ is the distance modulus derived from a recession velocity, $M_X^{\text{temp}}(t)$ is the template's magnitude at time t, $s_{(X)}$ is the stretch factor in the X band, $X_{\max}$ is the peak magnitude in the X band at the time of B-band maximum, σ_{obs} is the photometric error at the measurement, and σ_{template} is the error of the template at the epoch. We fit the parameters $t_{B\max}, s_{(X)}, X_{\max}$ to each set of curves of one SN. Although our equation (1) is expressed in magnitudes, we performed the fitting in linear scale. *U*-, *B*-, *V*-, *R*- and *I*-band light curves were treated with equal weights. We used the recession velocity of each host galaxy and cosmological parameters ($H_0 = 70.8\,\text{km s}^{-1}\,\text{Mpc}^{-1}, \Omega_{\text{M}} = 0.262, \Omega_\Lambda = 0.738$ from Spergel et al. 2007) to determine the distance modulus. Note that we did not introduce any colour terms in equation (1). We estimated the typical size of errors in our fitting procedure with Monte Carlo simulations. We fitted 30 artificial multiband light curves made from light-curve templates and obtained the dispersion for each fitted parameter.

In our Multiband Stretch method, the template can be applied to the observed light curve anywhere from -10 to $+80$ d after *B*-band maximum (-10 to $+70$ d for *U* band only). These ranges are wider than those of previous papers. For example, Goldhaber et al. (2001) used a range of -25 to $+50$ d. As a result, we can use information from later phases, especially around the second peak in the *R* and *I* bands.

3.3 *K*-corrections

Even though SNe Ia are simpler objects than galaxies, their *K*-corrections are not so simple since one must account for their spectral evolution. In this work, we define a *K*-correction as follows:

$$K_{X,t}^{\text{counts}} = 2.5 \log(1+z) + 2.5 \log \frac{\int \lambda F(\lambda, t) S_X(\lambda) \mathrm{d}\lambda}{\int \lambda F[\lambda/(1+z), t] S_X(\lambda)\,\mathrm{d}\lambda}. \quad (2)$$

Here, $F(\lambda, t)$ is the spectral energy distribution (SED) of the SN at time t, $S_X(\lambda)$ is the effective spectral transmission in the X band, and $K_{X,t}$ is the value of the K-correction at time t. See Kim, Goobar & Perlmutter (1996) and Nugent, Kim & Perlmutter (2002) for details. We used Bessell *U*-, *B*-, *V*-, *R*- and *I*-band filter shapes (cf. Bessell 1990) for the calculation.

Studies of *K*-corrections in nearby SN Ia samples go back to Hamuy et al. (1993). Kim et al. (1996) followed this work, and Nugent et al. (2002) provided a synthetic spectral library for SNe Ia. We used Nugent's model version1.1[3] for our calculations of *K*-corrections. There are three type of spectral models, named 'Branch normal', 'SN1991bg-like' and 'SN1991T-like' (Branch et al. 1993). We used the classification of each SN in Reindl et al. (2005) to choose a spectral model or used the 'Branch normal' spectral model when there was no spectral classification.

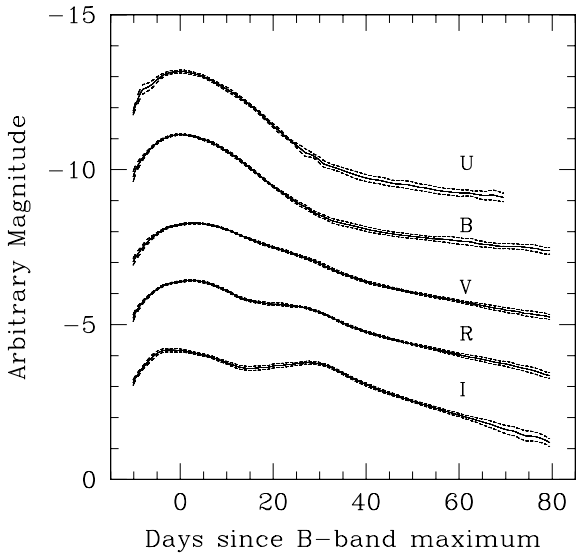

Figure 2. *U*-, *B*-, *V*-, *R*- and *I*-band light-curve templates (stretch factor = 1) with scatter. The rms (1σ) are derived from residuals of composite light curves and shown in dashed lines. The *B*-, *V*-, *R*- and *I*-band templates are from -10 to $+80$ d, and the *U*-band template is from -10 to 70 d after *B*-band maximum. The *U*-band template has larger dispersion than *B*-, *V*-, *R*- and *I*-band templates because *U*-band photometry is poorer than *B*-, *V*-, *R*- and *I*-band photometries.

3.4 Template

Fig. 2 shows our new *U*-, *B*-, *V*-, *R*- and *I*-band templates of SN Ia light curves. The templates were composed from 110 nearby ($z < 0.05$, 90 per cent have $z < 0.03$) SNe Ia light curves. The recipe to make the templates is as follows.

(i) Select a densely observed 'seed' light curve [we selected SN2001el (Krisciunas et al. 2003) for this work] and interpolate epochs.

[2]We did not need cross filter *K*-corrections because the typical redshift of our sample is so small.

[3]http://supernova.lbl.gov/∼nugent/nugent_templates.html

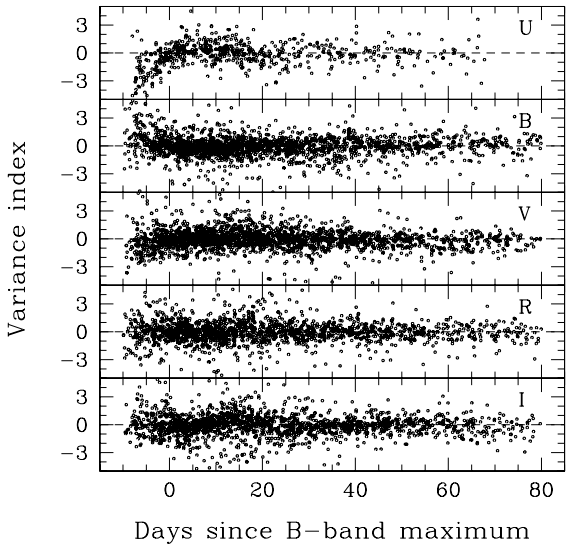

Figure 3. Residuals from light-curve template fitting in *U*-, *B*-, *V*-, *R*- and *I*-band magnitude. All epochs of 122 SNe Ia are plotted after fitting to the templates. Variance index is defined as $\Delta m_X/\sqrt{\sigma^2_{\rm template}+\sigma^2_{\rm photometry}}$, here, Δm_X is the residual between the *X*-band template and the observation (the plus sign means that photometry is fainter than template). $\sigma_{\rm template}$ and $\sigma_{\rm photometry}$ are typically of the order of 0.01 mag. Early phase *U*-band photometry (day <0) is systematically brighter than the template. A possible reason for the excess is *K*-correction.

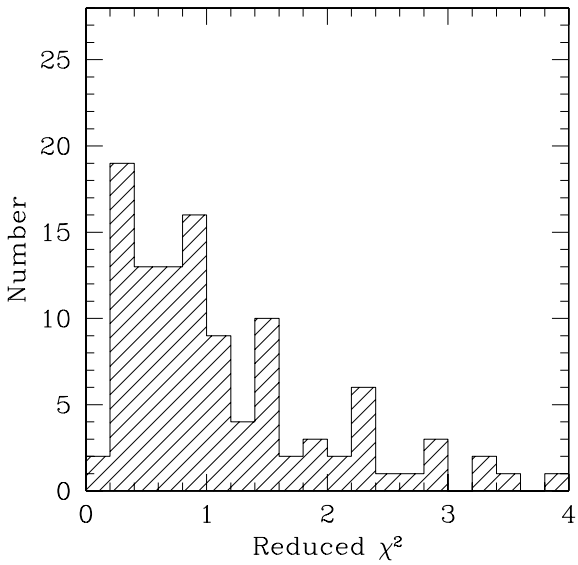

Figure 4. Distribution of reduced χ^2 of the fitting. Most of the SNe Ia well fit in the templates, but there are some SNe Ia not well fitted in the templates. χ^2/d.o.f. > 4: SN1994T, SN1996bo, SN1997cn, SN1998aq, SN1998de, SN1999ao, SN1999by, SN1999da, SN2002cx and SN2003du. χ^2/d.o.f. > 3: SN1992A, SN1992ag, SN1998bp and SN1999aw. A few of them are known as spectroscopically peculiar SNe Ia, but some of the others are known as 'Branch normal' SNe Ia.

(ii) Stretch the other 110 nearby SNe Ia light curves to fit in the current templates without *K*-corrections, then take the weighted average of all.

(iii) Iterate step (ii) until the templates become smooth.

(iv) Finally, stretch each template to fit in the $s = 1$ light curve defined by the Perlmutter et al. (1997) template.[4]

We did not apply *K*-corrections to make the light-curve template because well-observed SNe Ia which control the shape of the light-curve template are at the lowest redshift, and the size of the *K*-correction is smaller than typical photometric errors in all bands.

We calculated the residuals of each light curve from the template (see Fig. 2). We regard this scatter from the template as a result of the intrinsic diversity of SNe. The templates are available from our web site.[5]

4 RESULTS

Fig. 3 shows the size of typical residuals from the template light curves in *U*, *B*, *V*, *R* and *I* bands. Most of the observed light curves follow the templates closely. However, note that some early phase *U*-band photometry (day < 0) is systematically brighter than the template. This could be due to *K*-corrections (we made the templates by combining observed light curves without *K*-corrections, see Section 3.4).

However, there were a few SNe Ia which deviated significantly from the templates, due to an intrinsic peculiarity in their light-curve shapes or a failure to estimate their photometric errors properly. Peculiar light curves which do not follow the templates are very interesting for studies of the nature of SNe, but that is not our purpose in this paper. Therefore, we exclude 14/122 SNe Ia with reduced χ^2 values larger than three (see also Fig. 4) from further analysis. We did not exclude SNe Ia due to any other properties such as spectroscopic subtypes or host galaxy types. Only the exception is that we discuss those peculiar SNe in Section 4.3 related to *I*-band light curves. We refer to the remaining 108/122 SNe Ia in the following discussions. All parameters of this subset of 108 SNe Ia are given in Table 2. As we mentioned in Section 2, all of the 108 SNe have *B*- and *V*-band photometry, but they do not always have *U*-, *R*- and *I*-band photometry (see Table 1).

We also make some subsets of SNe Ia based on colours, stretch factors, host type and redshift in the following discussion. Those subsets are all made from the selected 108 SNe Ia.

4.1 Stretch factor

In Fig. 5, we show distributions of *U*-, *B*-, *V*-, *R*- and *I*-band stretch factors. The values in *V*, *R* and *I* bands are more concentrated than those in *U* and *B* bands. Since the *U*-band stretch factor suffers from larger errors than the *B*-band factor, due to many fewer measurements and larger photometric errors, we conclude that the *B*-band stretch factor is the best choice to serve as an index of SN Ia properties; we refer to it extensively in the following sections. Actually, we use the reciprocal of the *B*-band stretch factor in this paper in order more easily to compare our results with those of previous authors who used Δm_{15} as a light-curve shape parameter.

In Fig. 6, we compare our stretch factors with those of ALT04, using the common set of 58 SNe Ia. We obtain $s^{-1}_{(B)\rm Altavilla} = (0.86 \pm 0.07) \times s^{-1}_{(B)} + (0.13 \pm 0.07)$. The disagreement between our stretch factors and those of ALT04 may be due to the difference in time coverage of templates used in the light-curve fitting. We find the relationship between $\Delta m_{15}(B)$ and the inverse of our *B*-band stretch factor to be $\Delta m_{15} = (1.67 \pm 0.12) \times (s^{-1}_{(B)} - 1) + (1.13 \pm 0.02)$.

[4]http://supernova.lbl.gov/~nugent/nugent_templates.html
[5]http://www.ioa.s.u-tokyo.ac.jp/~takanashi/works/SN/template/

Table 2. The best-fitting parameters of 108 selected SNe Ia.

SN name	U	$s_{(U)}$	B	$s_{(B)}$	V	$s_{(V)}$	R	$s_{(R)}$	I	$s_{(I)}$	μ	$\frac{\chi^2}{\text{d.o.f.}}$	host	ref.
SN1989B	−18.61(0.03)	0.988(0.018)	−18.69(0.04)	0.902(0.021)	−18.98(0.02)	0.999(0.012)	−19.20(0.02)	0.944(0.020)	−19.26(0.02)	0.936(0.028)	30.89	0.476	–	(1)
SN1990O**	–	–	−19.41(0.02)	1.109(0.032)	−19.30(0.02)	1.138(0.024)	−19.29(0.03)	1.104(0.025)	−18.95(0.02)	1.061(0.026)	35.60	0.891	–	(2)
SN1990T	–	–	−18.92(0.06)	1.067(0.048)	−19.06(0.06)	0.995(0.032)	−18.95(0.03)	1.050(0.020)	−18.74(0.03)	1.006(0.017)	36.18	0.387	E	(2)
SN1990Y	–	–	−18.29(0.07)	1.076(0.054)	−18.67(0.09)	1.011(0.043)	−18.86(0.09)	0.954(0.045)	−18.79(0.17)	0.864(0.056)	35.95	1.445	E	(2)
SN1990af*	–	–	−18.91(0.01)	0.787(0.014)	−18.87(0.01)	0.789(0.011)	–	–	–	–	36.69	0.392	E	(2)
SN1991S	–	–	−19.32(0.13)	0.952(0.067)	−19.02(0.04)	1.096(0.034)	−19.00(0.03)	1.091(0.021)	−18.85(0.06)	0.996(0.039)	36.89	0.478	–	(2)
SN1991T	−21.26(0.02)	1.155(0.023)	−20.77(0.04)	1.119(0.025)	−20.92(0.02)	1.102(0.002)	−20.93(0.03)	1.092(0.030)	−20.73(0.04)	1.103(0.029)	32.34	2.363	–	(3)
SN1991U**	–	–	−19.26(0.06)	1.005(0.028)	−19.14(0.06)	1.102(0.032)	−19.17(0.03)	1.117(0.025)	−19.12(0.02)	0.989(0.024)	35.65	0.427	–	(2)
SN1991ag*	–	–	−19.41(0.02)	1.120(0.016)	−19.38(0.03)	1.110(0.014)	−19.38(0.03)	1.070(0.025)	−19.07(0.01)	1.065(0.014)	33.94	0.311	–	(2)
SN1992J	–	–	−18.69(0.07)	0.824(0.037)	−18.89(0.21)	0.784(0.111)	–	–	−18.55(0.03)	0.804(0.024)	36.44	0.543	–	(2)
SN1992K	–	–	−18.39(0.07)	0.590(0.036)	−18.60(0.23)	0.636(0.101)	–	–	−18.17(0.04)	0.801(0.022)	33.37	0.831	–	(2)
SN1992P**	–	–	−19.22(0.02)	1.035(0.020)	−19.11(0.01)	1.044(0.016)	–	–	−18.75(0.03)	1.127(0.057)	35.27	1.358	–	(2)
SN1992ae*	–	–	−19.09(0.06)	0.949(0.027)	−19.03(0.02)	0.942(0.020)	–	–	–	–	37.58	0.390	E	(2)
SN1992al**	–	–	−19.42(0.01)	0.984(0.014)	−19.28(0.01)	1.030(0.013)	−19.23(0.02)	1.002(0.011)	−18.93(0.01)	1.024(0.009)	33.88	0.292	–	(2)
SN1992aq**	–	–	−18.95(0.03)	0.840(0.034)	−18.82(0.02)	0.901(0.028)	–	–	−18.38(0.07)	0.818(0.050)	38.25	0.425	–	(2)
SN1992au*	–	–	−18.98(0.20)	0.785(0.061)	−18.91(0.19)	0.844(0.134)	–	–	−18.50(0.03)	0.798(0.025)	37.15	0.487	E	(2)
SN1992bc**	–	–	−19.60(0.03)	1.081(0.015)	−19.47(0.01)	1.039(0.034)	−19.41(0.03)	1.012(0.008)	−18.99(0.04)	1.027(0.017)	34.66	2.307	–	(2)
SN1992bg**	–	–	−19.21(0.04)	0.997(0.033)	−19.10(0.02)	1.025(0.014)	–	–	−18.78(0.03)	0.981(0.013)	35.89	0.677	–	(2)
SN1992bh	–	–	−18.84(0.02)	1.024(0.022)	−18.82(0.02)	1.044(0.022)	–	–	−18.58(0.02)	1.028(0.020)	36.44	0.402	–	(2)
SN1992bk*	–	–	−18.89(0.04)	0.796(0.029)	−18.83(0.05)	0.806(0.025)	–	–	−18.64(0.08)	0.740(0.045)	37.00	0.941	E	(2)
SN1992bl*	–	–	−19.03(0.03)	0.806(0.020)	−18.94(0.02)	0.836(0.013)	–	–	−18.62(0.02)	0.806(0.013)	36.34	1.117	E	(2)
SN1992bo*	–	–	−18.74(0.02)	0.773(0.011)	−18.69(0.02)	0.829(0.011)	−18.75(0.01)	0.781(0.006)	−18.52(0.01)	0.780(0.005)	34.49	0.761	E	(2)
SN1992bp	–	–	−19.43(0.02)	0.846(0.028)	−19.28(0.01)	0.912(0.018)	–	–	−18.81(0.03)	0.960(0.023)	37.69	1.547	E	(2)
SN1992br*	–	–	−18.56(0.07)	0.636(0.021)	−18.46(0.03)	0.741(0.028)	–	–	–	–	37.94	0.709	E	(2)
SN1992bs**	–	–	−18.94(0.04)	0.996(0.019)	−18.82(0.03)	1.015(0.015)	–	–	–	–	37.19	0.375	–	(2)
SN1993B**	–	–	−19.03(0.03)	0.930(0.023)	−18.89(0.01)	1.071(0.019)	–	–	−18.59(0.03)	1.018(0.029)	37.39	0.882	–	(2)
SN1993H	–	–	−18.38(0.02)	0.753(0.013)	−18.52(0.02)	0.793(0.007)	−18.59(0.01)	0.751(0.011)	−18.52(0.03)	0.719(0.012)	35.08	0.938	–	(2)
SN1993L	–	–	−17.74(0.07)	1.144(0.049)	−18.21(0.03)	1.009(0.018)	−18.34(0.04)	0.980(0.019)	−17.75(0.34)	1.138(0.149)	31.47	1.511	–	(4)
SN1993O**	–	–	−19.14(0.02)	0.955(0.018)	−19.01(0.02)	0.994(0.018)	–	–	−18.63(0.02)	0.992(0.029)	36.76	0.933	E	(2)
SN1993ac*	–	–	−18.95(0.04)	0.931(0.029)	−18.92(0.07)	0.909(0.043)	−18.87(0.02)	1.166(0.038)	−18.63(0.04)	1.067(0.042)	36.64	1.662	E	(5)
SN1993ae	–	–	−19.20(0.03)	0.838(0.022)	−19.23(0.04)	0.804(0.019)	−19.17(0.04)	0.797(0.021)	−18.97(0.02)	0.795(0.015)	34.55	0.360	–	(5)
SN1993ag	–	–	−18.86(0.02)	0.972(0.041)	−18.86(0.02)	0.992(0.025)	–	–	−18.54(0.04)	0.941(0.016)	36.68	0.988	E	(2)
SN1993ah	–	–	−19.19(0.09)	0.849(0.035)	−18.84(0.06)	1.117(0.045)	–	–	−18.81(0.02)	0.854(0.078)	35.50	1.926	–	(2)
SN1994D**	−18.99(0.02)	0.999(0.009)	−18.49(0.02)	0.838(0.010)	−18.38(0.01)	0.874(0.007)	−18.41(0.01)	0.835(0.008)	−18.07(0.02)	0.860(0.015)	30.24	2.570	E	(6)
SN1994M*	–	–	−18.73(0.02)	0.865(0.017)	−18.68(0.02)	0.920(0.013)	−18.86(0.02)	0.827(0.013)	−18.59(0.02)	0.851(0.010)	34.98	0.772	E	(5)
SN1994Q	–	–	−19.11(0.07)	1.103(0.057)	−19.12(0.07)	1.073(0.041)	−19.13(0.03)	1.131(0.028)	−18.83(0.02)	1.023(0.025)	35.47	0.250	E	(5)
SN1994S*	–	–	−19.39(0.02)	1.092(0.022)	−19.35(0.02)	1.045(0.026)	−19.28(0.02)	0.998(0.019)	−18.95(0.01)	1.064(0.024)	34.18	1.414	–	(5)

Table 2 – *continued*

SN name	U	$s_{(U)}$	B	$s_{(B)}$	V	$s_{(V)}$	R	$s_{(R)}$	I	$s_{(I)}$	μ	$\frac{\chi^2}{\text{d.o.f.}}$	host	ref.
SN1994ae	–	–	−18.68(0.01)	1.067(0.015)	−18.69(0.02)	1.067(0.017)	−18.79(0.01)	1.043(0.022)	−18.37(0.02)	1.105(0.023)	31.76	1.008	–	(7)
SN1995D**	–	–	−19.35(0.02)	1.081(0.012)	−19.24(0.01)	1.142(0.013)	−19.24(0.01)	1.104(0.009)	−18.91(0.01)	1.128(0.010)	32.55	0.361	E	(5)
SN1995E	–	–	−16.78(0.02)	0.992(0.028)	−17.43(0.02)	1.063(0.019)	−17.95(0.02)	0.968(0.017)	−18.12(0.02)	0.968(0.010)	33.49	0.390	–	(5)
SN1995ac*	–	–	−19.58(0.01)	1.072(0.013)	−19.52(0.01)	1.121(0.013)	−19.55(0.01)	1.063(0.010)	−19.33(0.01)	1.133(0.011)	36.68	1.524	–	(5)
SN1995ak	–	–	−18.85(0.07)	0.836(0.063)	−18.84(0.03)	0.927(0.022)	−19.03(0.02)	0.876(0.011)	−18.78(0.03)	0.959(0.015)	34.94	2.208	–	(5)
SN1995al	–	–	−18.74(0.02)	1.089(0.017)	−18.78(0.02)	1.117(0.015)	−18.78(0.02)	1.100(0.014)	−18.54(0.02)	1.112(0.011)	32.03	0.273	–	(5)
SN1995bd	–	–	−18.94(0.01)	1.177(0.011)	−19.21(0.01)	1.128(0.013)	−19.30(0.01)	1.157(0.015)	−19.01(0.01)	1.171(0.007)	34.17	2.178	–	(5)
SN1996C	–	–	−18.70(0.03)	1.089(0.013)	−18.72(0.02)	1.059(0.024)	−18.81(0.02)	1.023(0.017)	−18.47(0.01)	1.020(0.007)	35.32	0.781	–	(5)
SN1996X*	–	–	−19.63(0.01)	0.900(0.006)	−19.57(0.01)	0.941(0.007)	−19.56(0.01)	0.909(0.010)	−19.28(0.01)	0.981(0.014)	32.60	0.385	E	(5)
SN1996Z	–	–	−18.48(0.04)	0.936(0.031)	−18.73(0.02)	0.994(0.051)	−18.85(0.03)	0.868(0.072)	–	–	32.82	0.245	–	(5)
SN1996ab	–	–	−17.48(0.03)	0.990(0.038)	−17.54(0.03)	0.849(0.028)	–	–	–	–	37.08	1.052	–	(5)
SN1996ai	–	–	−14.19(0.01)	1.108(0.012)	−15.84(0.01)	1.090(0.011)	−16.62(0.01)	1.083(0.017)	−17.08(0.01)	1.053(0.011)	31.09	1.494	–	(5)
SN1996bk	–	–	−17.41(0.02)	0.906(0.013)	−17.96(0.01)	0.778(0.010)	−18.22(0.02)	0.699(0.007)	−18.31(0.02)	0.664(0.007)	32.42	2.158	E	(5)
SN1996bl*	–	–	−19.27(0.02)	1.005(0.016)	−19.21(0.02)	1.046(0.018)	−19.22(0.01)	1.060(0.017)	−18.98(0.01)	1.032(0.014)	35.95	1.014	–	(5)
SN1996bv	–	–	−19.01(0.02)	1.085(0.010)	−19.03(0.01)	1.180(0.006)	−19.16(0.02)	1.159(0.028)	−19.05(0.02)	1.061(0.012)	34.26	1.484	–	(5)
SN1997E	−19.06(0.02)	0.906(0.013)	−18.69(0.01)	0.835(0.007)	−18.70(0.01)	0.865(0.007)	−18.78(0.01)	0.816(0.007)	−18.55(0.01)	0.814(0.005)	33.78	0.794	E	(8)
SN1997Y**	−19.42(0.05)	0.938(0.062)	−19.01(0.02)	0.901(0.012)	−18.88(0.01)	1.000(0.012)	−18.94(0.01)	0.971(0.011)	−18.77(0.01)	0.978(0.009)	34.25	0.326	–	(8)
SN1997bp	−19.15(0.02)	1.232(0.022)	−19.11(0.01)	0.987(0.011)	−19.20(0.01)	1.166(0.011)	−19.27(0.01)	1.163(0.012)	−19.02(0.00)	1.058(0.007)	33.01	2.395	–	(8)
SN1997bq	−18.53(0.25)	1.224(0.180)	−18.82(0.09)	0.819(0.032)	−18.64(0.06)	1.085(0.077)	−18.78(0.04)	0.989(0.028)	−18.62(0.02)	0.949(0.019)	33.06	2.994	–	(8)
SN1997br	−19.75(0.02)	0.983(0.009)	−19.37(0.03)	0.845(0.016)	−19.31(0.01)	1.157(0.008)	−19.54(0.01)	1.043(0.007)	−19.48(0.01)	1.015(0.005)	32.66	2.555	–	(8)
SN1997cw	−18.75(0.21)	1.156(0.093)	−18.66(0.03)	0.967(0.023)	−18.66(0.02)	1.265(0.012)	−18.94(0.02)	1.153(0.016)	−18.91(0.01)	1.064(0.014)	34.39	0.830	E	(8)
SN1997dg**	−19.56(0.05)	0.920(0.052)	−19.03(0.02)	1.017(0.034)	−18.90(0.01)	1.027(0.016)	−18.99(0.02)	0.967(0.018)	−18.80(0.02)	0.908(0.024)	35.82	0.695	–	(8)
SN1997do*	−19.26(0.05)	1.061(0.032)	−18.95(0.02)	1.002(0.011)	−18.89(0.01)	1.137(0.011)	−18.97(0.01)	1.093(0.007)	−18.65(0.01)	1.113(0.006)	33.25	1.160	–	(8)
SN1997dt	–	–	−16.66(0.02)	0.971(0.009)	−17.07(0.02)	1.048(0.016)	−17.41(0.01)	1.048(0.012)	−17.59(0.01)	1.015(0.021)	32.08	2.996	–	(8)
SN1998D	–	–	−18.02(0.14)	0.904(0.091)	−18.25(0.27)	0.804(0.194)	−18.50(0.34)	0.735(0.110)	−17.60(0.06)	1.105(0.034)	31.3	0.067	–	(8)
SN1998V**	−19.73(0.02)	1.074(0.019)	−19.31(0.01)	1.012(0.007)	−19.20(0.00)	1.046(0.005)	−19.25(0.01)	1.031(0.008)	−19.02(0.01)	1.026(0.010)	34.33	0.877	–	(8)
SN1998ab**	−19.81(0.06)	1.015(0.037)	−19.35(0.02)	0.958(0.011)	−19.24(0.01)	1.107(0.006)	−19.36(0.01)	1.125(0.013)	−19.19(0.01)	1.054(0.014)	35.40	2.314	–	(8)
SN1998bu	−19.28(0.02)	1.147(0.009)	−19.09(0.01)	1.003(0.005)	−19.36(0.00)	1.013(0.003)	−19.54(0.01)	0.984(0.005)	−19.52(0.01)	1.006(0.004)	31.20	0.623	–	(8)
SN1998dh	−19.12(0.04)	1.043(0.021)	−18.71(0.01)	0.937(0.005)	−18.74(0.01)	1.006(0.006)	−18.82(0.01)	0.969(0.008)	−18.61(0.01)	0.963(0.005)	32.59	0.358	–	(8)
SN1998dk	−19.27(0.10)	1.016(0.071)	−18.73(0.03)	0.955(0.043)	−18.80(0.07)	1.036(0.039)	−18.88(0.01)	1.040(0.013)	−18.72(0.01)	1.012(0.013)	33.55	0.168	–	(8)
SN1998dm	−17.30(0.12)	1.282(0.062)	−17.16(0.03)	1.089(0.030)	−17.34(0.03)	1.150(0.015)	−17.54(0.02)	1.094(0.011)	−17.55(0.01)	1.085(0.009)	31.86	0.272	–	(8)
SN1998dx	−19.57(0.08)	0.805(0.043)	−19.12(0.03)	0.866(0.032)	−18.97(0.02)	0.880(0.028)	−19.04(0.02)	0.829(0.045)	−18.74(0.03)	0.942(0.079)	36.68	0.820	–	(8)
SN1998ec	−18.67(0.26)	1.176(0.109)	−18.52(0.04)	1.029(0.023)	−18.67(0.05)	1.008(0.024)	−18.66(0.02)	1.086(0.013)	−18.49(0.01)	1.048(0.018)	34.66	0.833	–	(8)
SN1998ef*	−19.89(0.02)	0.987(0.038)	−19.43(0.02)	0.904(0.012)	−19.36(0.01)	0.953(0.008)	−19.32(0.01)	0.976(0.016)	−19.16(0.01)	0.881(0.005)	34.27	1.006	–	(8)
SN1998eg*	−19.35(0.03)	0.954(0.058)	−18.93(0.02)	0.970(0.031)	−18.87(0.01)	0.974(0.031)	−18.94(0.01)	0.918(0.050)	−18.68(0.02)	1.927(0.340)	35.02	0.424	–	(8)
SN1998es	−19.75(0.02)	1.146(0.023)	−19.21(0.01)	1.132(0.016)	−19.26(0.01)	1.112(0.008)	−19.28(0.01)	1.102(0.015)	−18.99(0.01)	1.137(0.012)	33.05	0.708	–	(8)
SN1999X	−19.21(0.38)	1.075(0.133)	−19.05(0.14)	0.938(0.072)	−18.89(0.09)	1.007(0.074)	−18.86(0.06)	1.090(0.034)	−18.75(0.02)	0.928(0.064)	35.15	0.149	–	(8)
SN1999aa**	−19.91(0.03)	1.205(0.025)	−19.33(0.02)	1.143(0.026)	−19.22(0.03)	1.156(0.054)	−19.20(0.01)	1.136(0.014)	−18.89(0.01)	1.122(0.006)	34.06	1.248	–	(8)
SN1999ac*	−19.30(0.02)	1.092(0.026)	−19.01(0.01)	1.015(0.010)	−18.98(0.00)	1.069(0.004)	−19.03(0.00)	1.044(0.004)	−18.90(0.01)	0.991(0.003)	33.10	2.361	–	(8)
SN1999cc*	−19.13(0.03)	0.994(0.036)	−18.88(0.01)	0.850(0.012)	−18.80(0.01)	0.887(0.012)	−18.90(0.01)	0.843(0.010)	−18.66(0.02)	0.812(0.011)	35.66	0.751	–	(8)
SN1999cl	−17.28(0.02)	0.908(0.036)	−17.92(0.02)	0.972(0.019)	−19.03(0.01)	1.060(0.029)	−19.57(0.02)	1.005(0.136)	−19.79(0.02)	0.935(0.047)	32.83	0.631	–	(8)
SN1999cp**	–	–	−19.29(0.01)	1.075(0.005)	−19.18(0.01)	1.012(0.007)	−19.12(0.01)	1.042(0.011)	−18.79(0.01)	1.388(0.043)	33.21	2.162	–	(9)
SN1999dk*	–	–	−19.08(0.01)	1.099(0.013)	−19.05(0.00)	1.214(0.010)	−18.99(0.01)	1.240(0.017)	−18.76(0.01)	1.094(0.009)	33.87	2.868	–	(10)
SN1999dq	−19.94(0.01)	1.151(0.014)	−19.43(0.00)	1.094(0.004)	−19.45(0.00)	1.143(0.005)	−19.49(0.01)	1.119(0.006)	−19.28(0.01)	1.089(0.004)	33.82	1.443	–	(8)
SN1999ee	−18.62(0.12)	1.092(0.094)	−18.37(0.02)	1.124(0.016)	−18.60(0.08)	1.148(0.087)	−18.71(0.03)	1.095(0.035)	−18.50(0.04)	1.107(0.044)	33.25	1.498	–	(10)

Table 2 – *continued*

SN name	U	$s_{(U)}$	B	$s_{(B)}$	V	$s_{(V)}$	R	$s_{(R)}$	I	$s_{(I)}$	μ	$\frac{\chi^2}{\text{d.o.f.}}$	host	ref.
SN1999ef**	−19.04(0.10)	1.423(0.123)	−19.00(0.03)	1.037(0.021)	−18.86(0.02)	1.062(0.014)	−18.91(0.02)	1.024(0.023)	−18.49(0.03)	0.954(0.023)	36.05	1.270	–	(8)
SN1999ej*	−18.68(0.08)	0.845(0.051)	−18.33(0.03)	0.792(0.021)	−18.26(0.01)	0.863(0.026)	−18.32(0.02)	0.838(0.014)	−18.15(0.02)	0.781(0.020)	33.68	0.527	E	(8)
SN1999ek	–	–	−18.89(0.01)	0.954(0.010)	−18.92(0.01)	0.990(0.012)	−18.99(0.01)	0.935(0.014)	−18.82(0.01)	0.892(0.006)	34.38	0.837	–	(10)
SN1999gd	−17.54(0.07)	1.123(0.069)	−17.64(0.02)	0.942(0.010)	−17.97(0.01)	0.984(0.010)	−18.23(0.02)	0.956(0.014)	−18.24(0.02)	0.948(0.013)	34.57	1.518	–	(8)
SN1999gh	−19.01(0.12)	0.773(0.049)	−18.62(0.02)	0.756(0.016)	−19.12(0.03)	0.595(0.008)	−19.07(0.01)	0.659(0.005)	−18.82(0.01)	0.692(0.004)	32.86	0.946	E	(8)
SN1999gp*	−19.80(0.02)	1.186(0.022)	−19.22(0.01)	1.204(0.008)	−19.19(0.00)	1.236(0.006)	−19.21(0.01)	1.241(0.007)	−18.89(0.01)	1.208(0.019)	35.23	1.849	–	(8)
SN2000B	−19.16(0.14)	0.968(0.063	−18.90(0.03)	0.854(0.029)	−19.14(0.06)	0.778(0.020)	−19.00(0.01)	0.876(0.009)	−18.67(0.01)	0.885(0.016)	34.58	0.638	E	(8)
SN2000E	−18.85(0.01)	1.166(0.011)	−18.52(0.00)	1.101(0.003)	−18.62(0.00)	1.101(0.003)	−18.66(0.00)	1.102(0.006)	−18.51(0.01)	1.057(0.005)	31.31	2.699	–	(11)
SN2000bh*	–	–	−19.02(0.03)	0.995(0.017)	−18.97(0.01)	1.043(0.007)	−19.00(0.02)	1.029(0.007)	−18.63(0.02)	1.025(0.005)	34.95	0.383	–	(12)
SN2000bk	–	–	−18.22(0.01)	0.766(0.006)	−18.44(0.01)	0.750(0.004)	−18.50(0.00)	0.748(0.004)	−18.35(0.01)	0.732(0.003)	35.18	1.158	E	(10)
SN2000ca**	−20.08(0.03)	1.142(0.033)	−19.46(0.01)	1.118(0.009)	−19.33(0.01)	1.080(0.007)	−19.29(0.01)	1.067(0.006)	−18.90(0.01)	1.065(0.005)	35.02	1.951	–	(12)
SN2000ce	−17.08(0.14)	1.313(0.098)	−17.26(0.06)	1.035(0.035)	−17.66(0.04)	1.077(0.034)	−17.95(0.07)	1.151(0.088)	−18.02(0.03)	1.138(0.088)	34.21	0.307	–	(8)
SN2000cf*	−18.97(0.14)	0.987(0.120)	−18.91(0.03)	0.873(0.017)	−18.82(0.01)	0.937(0.015)	−18.91(0.02)	1.078(0.049)	−18.57(0.01)	1.066(0.042)	35.95	0.473	–	(8)
SN2000cn	−18.44(0.03)	0.974(0.025)	−18.44(0.01)	0.761(0.009)	−18.53(0.01)	0.835(0.011)	−18.62(0.01)	0.808(0.019)	−18.41(0.01)	0.769(0.017)	34.98	1.126	–	(8)
SN2000cx	−19.70(0.07)	1.138(0.087)	−19.34(0.06)	0.863(0.055)	−19.41(0.10)	0.746(0.046)	−19.29(0.06)	0.766(0.029)	−18.87(0.04)	0.807(0.018)	32.40	0.220	E	(8)
SN2000dk*	−19.22(0.01)	0.805(0.011)	−18.87(0.01)	0.762(0.008)	−18.83(0.01)	0.836(0.006)	−18.90(0.01)	0.789(0.007)	−18.57(0.01)	0.777(0.020)	34.21	1.792	E	(8)
SN2001V	–	–	−19.56(0.02)	1.174(0.021)	−19.58(0.03)	1.153(0.043)	−19.57(0.02)	1.151(0.024)	−19.35(0.02)	1.123(0.025)	34.17	1.319	–	(13)
SN2001ba**	–	–	−19.41(0.01)	1.043(0.008)	−19.28(0.01)	1.030(0.012)	–	–	−18.85(0.01)	1.016(0.010)	35.61	0.888	–	(12)
SN2001bt	–	–	−18.71(0.01)	0.899(0.007)	−18.82(0.00)	1.006(0.003)	−18.95(0.01)	0.962(0.009)	−18.75(0.01)	0.954(0.009)	33.97	0.630	–	(3)
SN2001cn	–	–	−18.88(0.01)	0.950(0.007)	−18.94(0.01)	1.026(0.003)	−19.04(0.01)	0.969(0.004)	−18.77(0.01)	0.975(0.004)	34.10	0.561	–	(3)
SN2001cz	–	–	−19.18(0.01)	1.056(0.012)	−19.22(0.01)	1.058(0.008)	−19.26(0.01)	0.998(0.017)	−18.98(0.01)	1.039(0.010)	34.23	0.810	–	(3)
SN2001el	−18.20(0.01)	0.993(0.017)	−18.14(0.01)	0.953(0.012)	−18.20(0.01)	1.090(0.014)	−18.38(0.01)	0.993(0.006)	−18.09(0.01)	1.060(0.011)	30.92	1.128	–	(14)
SN2001en	−18.83(0.13)	1.241(0.436)	−18.79(0.01)	0.953(0.007)	−18.86(0.01)	1.027(0.007)	−18.96(0.01)	0.971(0.004)	−18.69(0.01)	0.976(0.005)	34.03	0.542	–	(15)
SN2002bo	–	–	−17.92(0.02)	0.951(0.024)	−18.25(0.01)	0.991(0.009)	−18.51(0.04)	1.007(0.027)	−18.37(0.01)	0.997(0.007)	31.85	0.907	–	(3)
SN2004S	–	–	−18.93(0.02)	0.946(0.016)	−18.78(0.03)	1.103(0.017)	−18.88(0.02)	0.990(0.012)	−18.65(0.02)	0.997(0.011)	33.00	0.479	–	(16)

List of parameters of 108 selected SNe Ia used in this paper. ∗ means 'BV bluer' SNe Ia and ∗∗ means 'BV bluest' SNe Ia (see Section 4.2). SNe Ia hosted by E or S0 galaxies are listed as 'E'. References are as follows: (1) Wells et al. (1994), (2) Hamuy et al. (1996a), (3) Krisciunas et al. (2004b), (4) Altavilla et al. (2004), (5) Riess et al. (1999a), (6) Richmond et al. (1995), (7) Riess et al. (2005), (8) Jha et al. (2006), (9) Krisciunas et al. (2000), (10) Krisciunas et al. (2001), (11) Valentini et al. (2003), (12) Krisciunas et al. (2004a), (13) Vinko et al. (2003), (14) Krisciunas et al. (2003), (15) VSNET and (16) Kuntal et al. (2005).

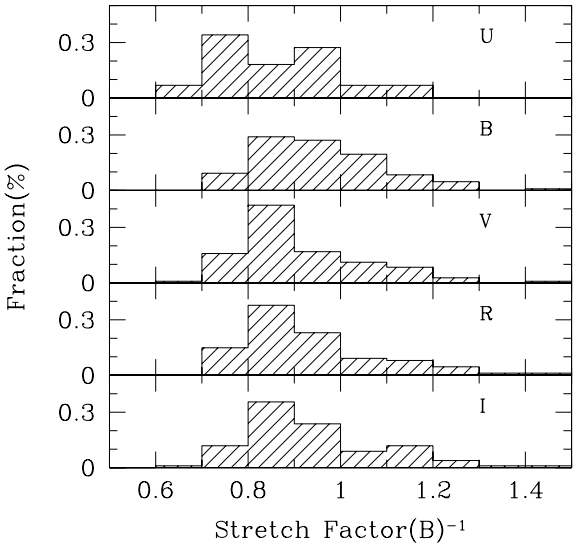

Figure 5. Histograms of the stretch factors in the *U*, *B*, *V*, *R* and *I* bands. There are 44 SNe Ia in the *U* band, 108 SNe Ia in the *B* band, 108 SNe Ia in the *V* band, 88 SNe Ia in the *R* band and 102 SNe Ia in the *I* band.

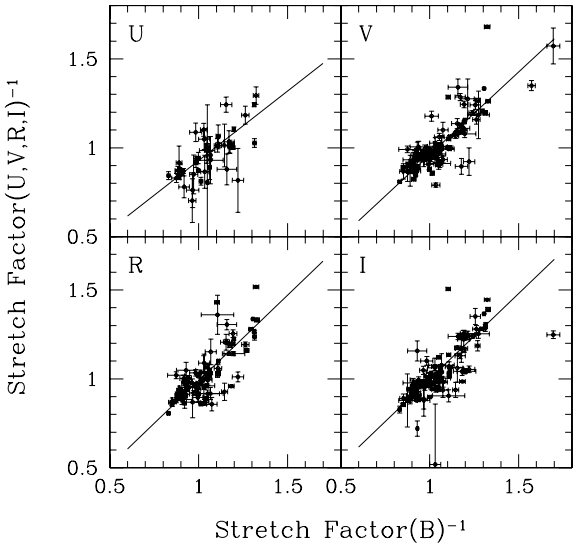

Figure 7. Relations between the inverse *B*-band stretch factor and inverse *U*-, *V*-, *R*- and *I*-band stretch factors of all SNe Ia. The solid lines are regression lines (see also Table 3).

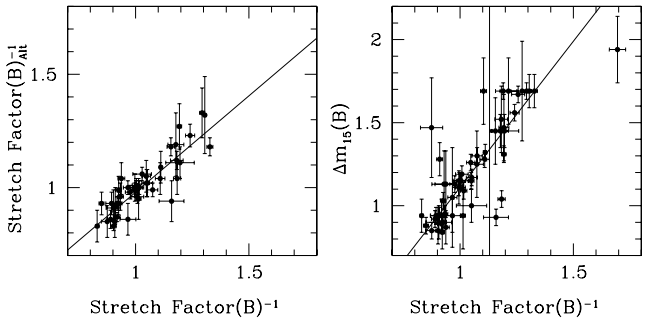

Figure 6. Comparison with ALT04. The left-hand panel shows a relation between inverse *B*-band stretch factors. The right-hand panel shows the relation between the inverse *B*-band stretch factor (this work) and Δm_{15} from ALT04. The solid line is a regression line derived from least χ^2 fitting.

Table 3. Relationships between inverse *B*-band stretch factor and stretch factors in *U*, *V*, *R* and *I* bands.

Band	Relation	rms (mag)	Number
U band	$(0.78 \pm 0.07) \times s_{(B)}^{-1} + (0.14 \pm 0.07)$	0.040	44
V band	$(0.93 \pm 0.05) \times s_{(B)}^{-1} + (0.03 \pm 0.05)$	0.009	108
R band	$(1.04 \pm 0.05) \times s_{(B)}^{-1} - (0.05 \pm 0.05)$	0.009	88
I band	$(1.02 \pm 0.05) \times s_{(B)}^{-1} - (0.01 \pm 0.06)$	0.011	102

This result is consistent with ALT04, which found $\Delta m_{15} = (1.98 \pm 0.16) \times (s^{-1}_{(B)\rm Altavilla} - 1) + (1.13 \pm 0.02)$.

Fig. 7 shows the relationship between the inverse *B*-band stretch factor and the inverse *U*-, *V*-, *R*- and *I*-band stretch factors. The best-fitting relations are listed in Table 3. JHA06 showed that relations among *U*-, *B*- and *V*-band stretch factors are consistent with a 'universal' stretch, and our results agree: our *B*-, *V*-, *R*- and *I*-band stretch factors are equal within the formal uncertainties. However, the coefficient of the relationship between *U*- and *B*-band stretch factors is smaller than those for the relationships between *B*-, *V*-, *R*- and *I*-band stretch factors. If we select 19 SNe Ia in common with JHA06, the relation between *U*- and *B*-band stretch factors is $s_{(U)} = (1.03 \pm 0.11) \times s_{(B)} + (0.05 \pm 0.11)$. This result is consistent with those of JHA06 ($s_{(U)} = 1.04 \times s_{(B)} - 0.02$).

4.2 Magnitude and colour

Fig. 8 shows the distribution of *U*-, *B*-, *V*-, *R*- and *I*-band absolute peak magnitudes corrected for Galactic extinction according to Schlegel et al. (1998). The trend that redder bands are more concentrated than bluer bands possibly indicates the effects of extinction by dust (see also Table 4).

The colours of the SNe Ia also suggest that dust plays an important role. Fig. 9 shows the distribution of the $(B - V)$ colour at the time of *B*-band maximum, $(B - V)_{\rm max}$. The tail of the redder side in Fig. 9 is likely SNe Ia reddened by dust in their host galaxies. As shown in Fig. 10, redder SNe Ia tend to be missing at higher redshift, implying that the redder SNe Ia are affected by dust. The clear edges of the blue side of the distributions in Figs 9 and 10 indicate that the $(B - V)_{\rm max}$ colour of bluest SNe Ia is almost constant. Fitting a single-sided Gaussian to the left-hand side of the histogram in Fig. 9 [$(B - V)_{\rm max} > -0.20$], we estimate the intrinsic colour of bluest SN Ia as $(B - V)_{\rm max} = -0.12$. Fig. 11 shows relationships between $(B - V)_{\rm max}$ and the other colours at the time of *B*-band maximum. We will discuss this in detail in Section 5.

We should pay attention to the possibility that there are intrinsically redder SNe Ia. We cannot distinguish those redder SNe Ia from the SNe Ia reddened by host galaxy dust based on apparent colour. In Sections 6 and 7, we discuss the issue.

Based on the result of single-side Gaussian fitting of the $B - V$ distribution, we made three subsamples, 'BV bluest' SNe Ia [$-0.14 < (B - V)_{\rm max} \leq -0.10$, -0.12 ± 0.02 mag around the median], 'BV bluer' SNe Ia [$-0.10 < (B - V)_{\rm max} < -0.02$, 0.1 mag redder than the median] as less dust-affected samples and 'BV redder' SNe Ia [$0.00 < (B - V)_{\rm max}$] as a dust-affected sample. We use them in the following discussions.

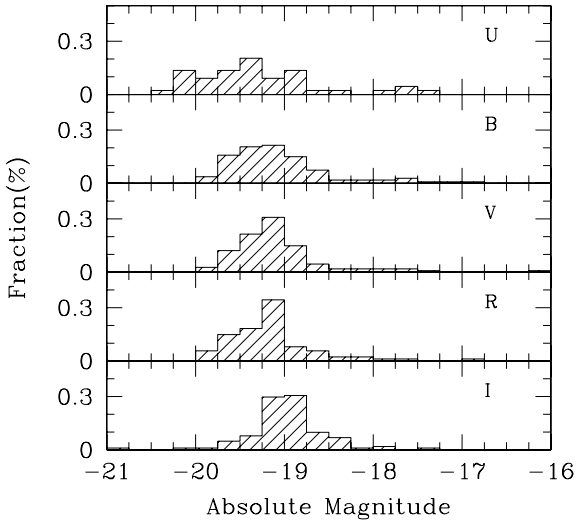

Figure 8. Histograms of absolute magnitudes in U, B, V, R and I bands. The magnitudes are corrected for Galactic dust extinction, but not for host galaxy dust extinction. Bluer bands such as U and B band have broader distributions than redder bands.

Table 4. Average absolute magnitudes (rms) and stretch factors (rms).

	Magnitude	Stretch factor	Number
U band	−19.08 (0.79)	1.07 (0.14)	44
B band	−18.79 (0.76)	0.96 (0.12)	108
V band	−18.84 (0.58)	1.00 (0.13)	108
R band	−18.93 (0.53)	1.00 (0.13)	88
I band	−18.70 (0.45)	0.98 (0.15)	102

4.3 *I*-band peculiarity

It is well known that there is quite a variety of shapes in the I-band light curves of SNe Ia. Usually, there is a 'bump' or a 'second peak' in the I band, but some SNe Ia do not have a secondary peak (see Fig. 12). Some previous authors fitted these I-band light curves using two Gaussian functions (Contardo, Leibundgut & Vacca 2000; Nobili et al. 2005). However, we tried to fit I-band light curves using only one template to avoid introducing extra parameters.

From all of the 122 SNe Ia, we selected 71 well-observed SNe Ia which have at least one I-band measurement in two periods, −10 to 0 d and +10 to +20 d. Based on photometry during these periods, the 71 SNe Ia were classified into two types; normal I-band light curves and peculiar I-band light curves (see Fig. 13), where 'peculiar' means that the I-band light curves are fainter than the I-band template from −10 to 0 d and brighter than the I-band template from +10 to +20 d.

We found about 90 per cent of SNe Ia (63/71 SNe) can be fitted well with the template and only eight SNe Ia (SN1991bg, SN1995ac, SN1997br, SN1998ab, SN1999ac, SN1999by, SN1999gh and SN2002cx) cannot be fitted well with the template. Most of those which deviate from the template are known to be spectroscopically peculiar as well. For example, SN1991bg and SN1999by are classified as 'SN1991bg-like', whereas SN1995ac and SN1997br are classified as 'SN1991T-like', and SN2002cx is known as a very peculiar SN Ia (Li et al. 2003). On the other hand, I-band light curves of SN1991T and SN1995bd, which are classified spectroscopically as 'SN1991T-like', do fit the I-band light template. Based on the value of reduced χ^2 calculated with the Multiband Stretch method, these SNe which do not fit the template I-band light curve have been excluded from the samples in the following discussions, as we mentioned in the beginning of Section 4. As Nobili et al. (2005) pointed out the correlation between lack of a second I-band maximum and a lower B-band stretch, the Multiband Stretch method would have room for improvement in the treatment of these SNe.

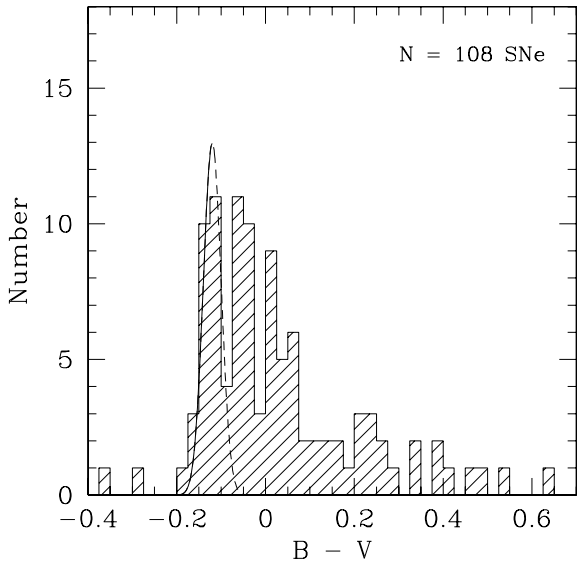

Figure 9. Rest-frame distribution of $(B-V)_{\rm max}$ without host galaxy dust correction. The tail on the redder side can be attributed to host galaxy dust reddening. Bluer SNe Ia may be less affected by host galaxy dust. The median $(B-V)_{\rm max}$ of one-side Gaussian fit using only bluest SNe Ia is -0.12 ± 0.02. This value is consistent with ALT04.

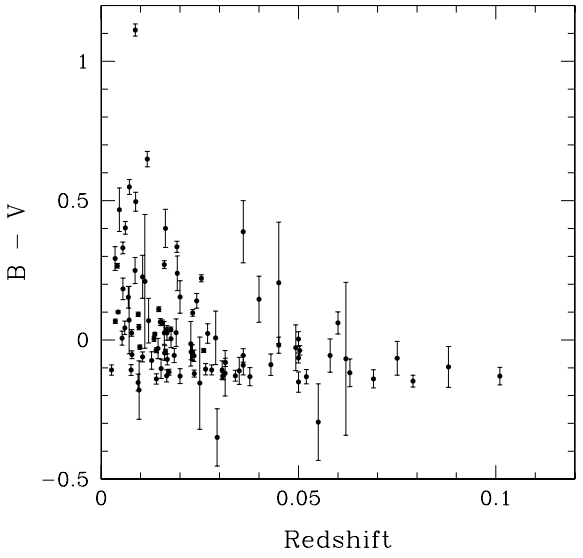

Figure 10. $(B-V)_{\rm max}$ distribution as a function of redshift. Error bars include only photometric errors and fitting errors (peculiar velocities of galaxies are not included). Redder SNe Ia tend to be missing at larger redshift because they are fainter than bluer SNe Ia which expected to be free from host galaxy dust. Also this figure shows there is no apparent trend in the bluest end of $(B-V)_{\rm max}$ colour with redshift at the range of $z \lesssim 0.1$.

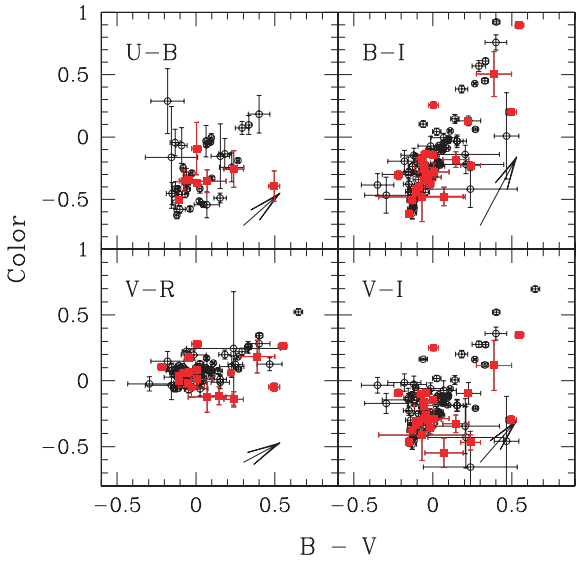

Figure 11. Colour–colour diagram of SNe Ia at B-band maximum. Filled red squares are SNe Ia hosted by E or S0 galaxies. Arrows show direction and size of reddening when we assume that the absorption properties of host galaxy dust are the same as Galactic dust ($R_U = 5.434, R_B = 4.315, R_V = 3.315, R_R = 2.673, R_I = 1.940$ from Schlegel et al. 1998) and $A_B = 1.0$ mag. Even if we selected only SNe Ia hosted by elliptical galaxies, they are plotted along the Galactic dust reddening direction. The colours have been corrected for Galactic dust reddening, but not for host galaxy dust reddening.

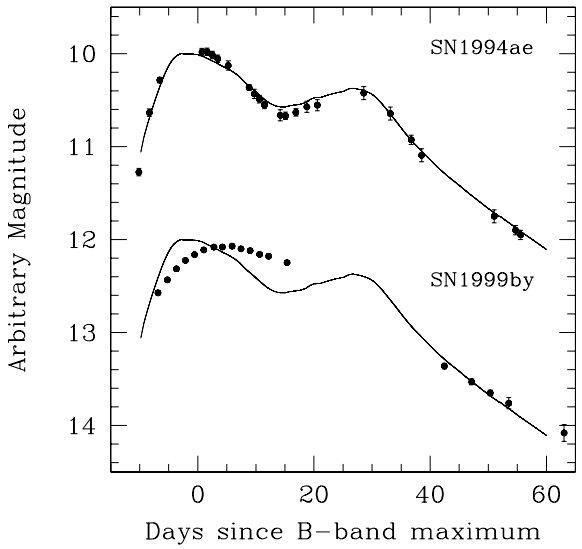

Figure 12. Examples of a normal I-band light curve and a peculiar I-band light curve. SN1994ae is a spectroscopically normal SN Ia, and there is a 'bump' in the I-band light curve. SN1999by is a spectroscopically peculiar SN Ia, and there is no 'bump' in the I-band light curve.

5 SUBGROUP OF SNe IA

Do all SNe Ia with the same B-band stretch factor have the same intrinsic colours? The best way to answer this question is to compare a series of well-calibrated spectra from different events, but we lack such a data set. Therefore, we have investigated the issue using photometric information from our sample of SNe Ia.

In Fig. 14, we plot SNe Ia classified on the basis of their $(B - V)_{\max}$ colour as 'BV bluest' SNe Ia, 'BV redder' SNe Ia and 'others'. As we discussed in Section 4, the bluer SNe Ia may be free from dust extinction. In Fig. 14, there is a 'sub' group at the lower right, with an inverse B-band stretch factor of > 1.1 and $(V - I)_{\max} < 0$. This 'sub' group consists of SNe Ia which are redder in $(B - V)_{\max}$, though they are bluer in $(V - I)_{\max}$. It is difficult to explain this combination of colours using ordinary SNe Ia shining through dust in their host galaxies. Instead, it may mean that the 'sub' group is due to a set of SNe Ia with intrinsic SEDs which differ from the 'main' group with inverse B-band stretch factor <1.1, at least in B, V and I bands.

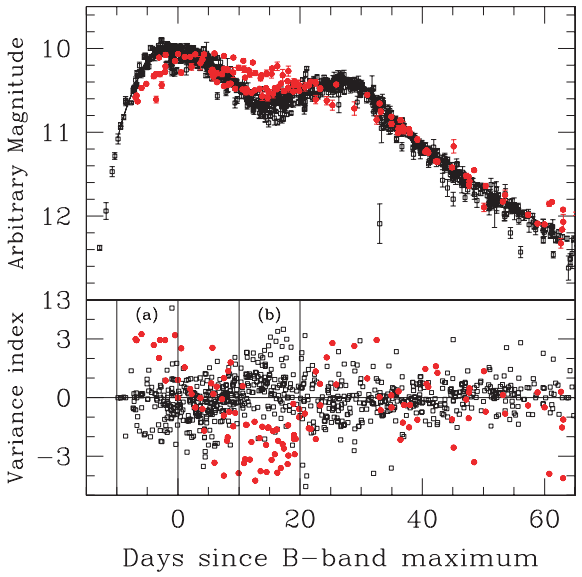

Figure 13. I-band light curves of 71 selected SNe Ia (top panel) and distribution of the epochs (bottom panel). Variance index is defined as $\Delta m_I / \sqrt{\sigma^2_{\text{template}} + \sigma^2_{\text{photometry}}}$, where Δm_I is the residual between the I-band template and the observation, $\sigma_{\text{photometry}}$ is the photometric error and σ_{template} is the template error. We classified the SNe into two types, normal I-band light curves (open squares) and peculiar I-band light curves (filled red circles), according to photometry points (see text).

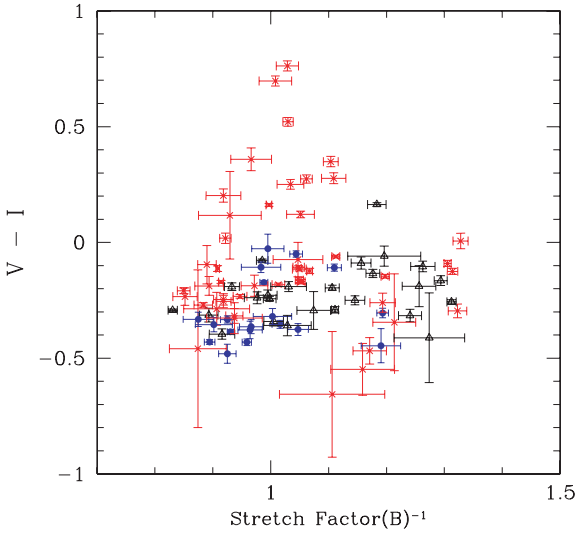

Figure 14. Distribution of $(V - I)_{\max}$ as a function of the inverse B-band stretch factor. Filled blue circles are 'BV bluest' SNe Ia, red crosses are 'BV redder' SNe Ia and open triangles are the other SNe Ia.

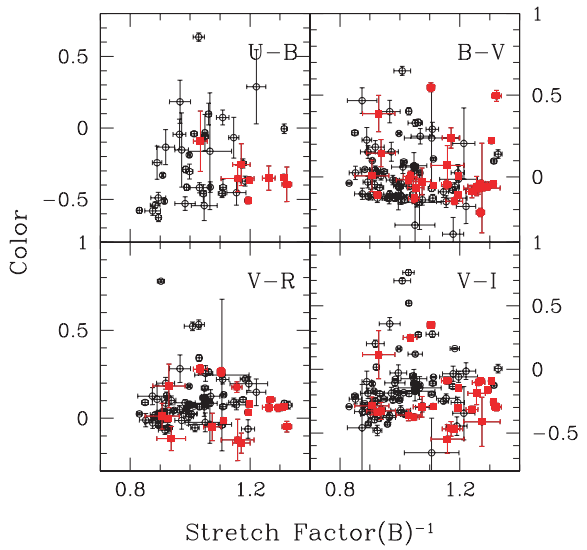

Figure 15. Distribution of rest-frame colours as a function of the inverse *B*-band stretch factor. Filled red squares are SNe hosted by E or S0 galaxies. The colours have been corrected for Galactic dust reddening, but not for host galaxy dust reddening.

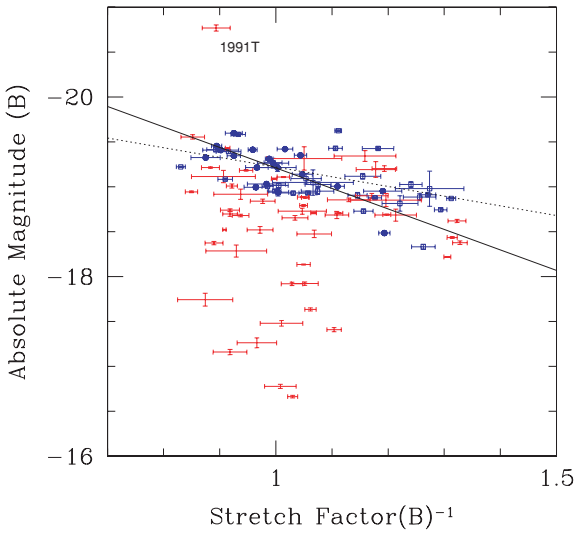

Figure 16. Relations between inverse *B*-band stretch factor and absolute *B*-band magnitude. Filled blue circles are 'BV bluest' SNe Ia, open blue squares are 'BV bluer' SNe Ia and the other symbols are for other SNe Ia. The solid line is a relation between inverse *B*-band stretch factor and *B*-band magnitude derived from 'BV bluest' SNe Ia, while the dashed line is a relation derived from 'BV bluest' + 'BV bluer' SNe Ia. Redder and fainter SNe Ia than those 'BV bluest' or 'BV bluer' SNe Ia may be affected by host galaxy dust.

There are some observational indications that properties of SNe Ia are related to their environment. Hamuy et al. (1996a) showed that the mean luminosity of SNe Ia in elliptical galaxies is fainter than that of SNe Ia in spiral galaxies. Mannucci et al. (2005) and Sullivan et al. (2006) also showed that the star-forming activity in a galaxy is related to properties of its SNe Ia. We have plotted the SNe Ia hosted by E or S0 galaxies in Fig. 15. We note that the SNe Ia of the 'sub' group at the lower right tend to be found in E or S0 galaxies. However, not all SNe Ia found in E or S0 galaxies belong to this group.

Of course, a difference of intrinsic colours does not mean a difference of intrinsic luminosity directly. However, a difference in intrinsic colours affects the accuracy of correcting for host galaxy dust extinction if we correct the extinction according to the apparent colour of the SN Ia. For example, the bluer SNe Ia with inverse *B*-band stretch factors >1.2 in the $(B-V)$ panel of Fig. 15 are redder than the bluer SN Ia with inverse *B*-band stretch factors <1.2 by about 0.05 mag in $(B-V)_{\rm max}$. If we treat the $(B-V)_{\rm max}$ as a constant when we estimate the host galaxy dust extinction, the correction will be overestimated systematically by about 0.2 mag in the *B* band. This is critical if we want to use SNe Ia as distance indicators for cosmological studies.

6 RELATIONS BETWEEN *B*-BAND STRETCH FACTOR AND BRIGHTNESS

Figs 16 and 17 show the relationships between inverse *B*-band stretch factor and luminosity at the *B*-band maximum (hereafter, stretch–magnitude relation) in *U*, *B*, *V*, *R* and *I* bands. The scatter in the luminosity is mainly caused by three factors: the peculiar velocity of the host galaxy, extinction by dust in the host galaxy and intrinsic diversity of SNe Ia.

Peculiar velocity makes the dispersion larger when we estimate the distance to a SN from its host's recession velocity. The effect of peculiar velocity must be treated properly if the host galaxy is nearby. For example, if a host galaxy has a peculiar velocity of 400 km s^{-1}, we will overestimate or underestimate the luminosity of its SN by $\sim$0.3 mag at $z=0.01$ and $\sim$0.1 mag at $z=0.02$. However, statistically speaking, the effect can be small if the sample size is large enough. In our case, Table 5 shows that there is no significant effect on averaged absolute magnitudes caused by peculiar velocity if we choose 'BV bluest' + 'BV bluer' SNe Ia in order to avoid the effect of host galaxy dust extinction. In Fig. 18, we plot individual SNe Ia shown in Table 5, however, there are no considerable effects caused by peculiar velocities. Table 5 also shows that the scatter

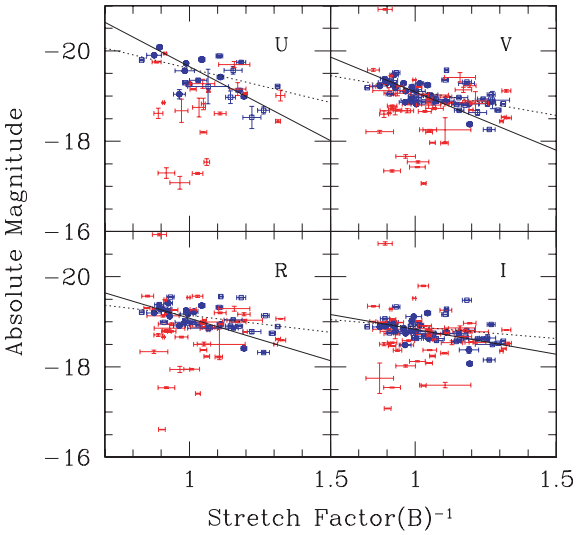

Figure 17. Relations between inverse *B*-band stretch factor and absolute magnitude of *U*, *V*, *R* and *I* bands. Filled blue circles are 'BV bluest' SN Ia, open blue squares are 'BV bluer' SNe Ia and the other symbols are for other SNe Ia. The solid line is a relation between inverse *B*-band stretch factor and *B*-band magnitude derived from 'BV bluest' SNe Ia, while the dashed line is a relation derived from 'BV bluest' + 'BV bluer' SNe Ia.

Table 5. Average magnitudes of 'BV bluest' + 'BV bluer' SNe Ia at different redshifts.

Redshift	M_B	Number
$0.00 < z \leq 0.02$	−19.13 (0.35)	18
$0.02 < z \leq 0.05$	−19.15 (0.23)	19
$0.05 < z$	−19.01 (0.26)	10

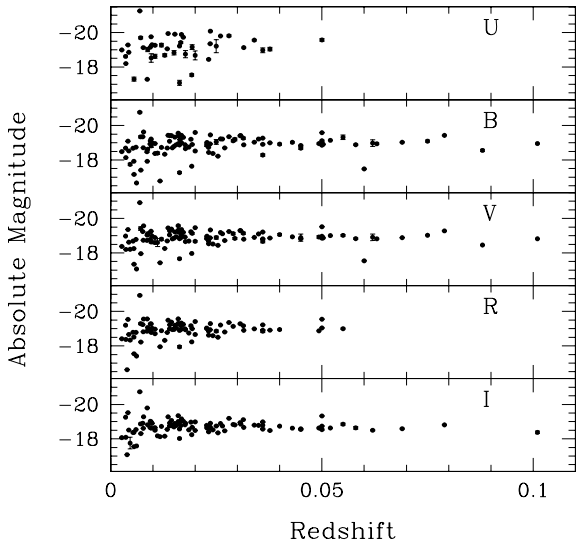

Figure 18. Absolute magnitude distribution as a function of redshift. Magnitude is corrected for Galactic dust extinction, but not for host galaxy dust extinction. The bright outlier near $z = 0.007$ is SN1991T. If peculiar velocity is not negligible, the number of brighter SNe Ia than the average increases at lower z (also fainter SNe Ia increase, but we cannot distinguish them from the SNe Ia which suffer extinction by host galaxy dust). However, there is no considerable effect caused by peculiar velocity. See also Table 5.

size in the nearest sample ($0.00 < z \leq 0.02$) is only 10 per cent larger than the further samples.

It is better to include properly the effect of peculiar velocity in error bars, however, we do not know which value could represent peculiar velocities. For example, the peculiar velocity of galaxies in the clusters often reaches $\sim$1000 km s^{-1}. It is very difficult to estimate the appropriate value of peculiar velocities without additional observations, and we do not want to unnecessarily overestimate the size of error bars.

One way to avoid the peculiar velocity problem is to use further redshift SNe Ia only. But, the number of SNe Ia becomes smaller in compensation for the selection. Hence, we did not make any corrections for the effect of peculiar velocity in this study.

Extinction due to dust in the host galaxy is a major contributor to the scatter in luminosity. Unfortunately, it is very difficult to estimate this extinction properly. We must separate the effect of host galaxy dust extinction from intrinsic colour variations of SNe Ia. One way to avoid this problem is to use only bluer SNe Ia which are expected to be free from extinction. In Fig. 16, we plot the 'BV bluest' SNe Ia and 'BV bluer' SNe Ia samples. Coefficients of the relationship between absolute magnitude and inverse stretch factor are listed in Table 6. In all passbands, the slope of the line derived from the 'BV bluest' sample is about double that of the slope of the line derived from the combined 'BV bluest' + 'BV bluer' sample. Figs 16 and 17 also show that most of the 'BV bluest' SNe have broader light-curve widths than 'BV bluer' SNe. This suggests there may be different groups of SNe Ia with different intrinsic properties. The slope of the stretch–magnitude relation of ALT04 is 1.83 [using 1.102 in table 1 of Altavilla's paper and $\Delta m_{15} = (1.67 \pm 0.12) \times (s_{(B)}^{-1} - 1) + (1.13 \pm 0.02)$], which is shallower than the slope of 'BV bluest' SNe Ia but steeper than the slope of the combined 'BV bluest' + 'BV bluer' sample.

We also tried to compare the dispersion of luminosity of 'BV bluest' SNe Ia around the stretch–magnitude relation derived from 'BV bluest' SNe Ia with that of SNe Ia hosted by E or S0 galaxies. Those SNe Ia hosted by E or S0 galaxies should be largely free from extinction due to interstellar dust in the host galaxy, but Fig. 19 shows that they have a larger dispersion than 'BV bluest' SNe Ia (which are also expected to be free from host galaxy dust extinction), see also Table 7. Even if we select 'BV bluer' SNe Ia hosted by E or S0 galaxies, the dispersion is still larger than 'BV bluest' SNe Ia without any dust/colour corrections. These facts may indicate that SNe Ia hosted by E or S0 galaxies have larger intrinsic diversity than SNe Ia hosted by other type of galaxies, or that the host galaxies have some significant dust extinction.

Of course, the scatter of brightness of SNe Ia in E or S0 galaxies could be attributed to the peculiar velocity of the host galaxies, but the peculiar velocity of host galaxies cannot account for the fact that the direction of the distribution of SNe Ia hosted by E or S0 galaxies shown in Fig. 11 is parallel to the direction of the distribution due to dust in the Milky Way.

Table 6. Relationships between *B*-band stretch factor and luminosity.

	Sample	Relation	rms (mag)	Number
U band	6A	$(3.28 \pm 0.40) \times s_{(B)}^{-1} - (22.93 \pm 0.42)$	0.32	8
	6B	$(1.50 \pm 0.40) \times s_{(B)}^{-1} - (21.11 \pm 0.44)$	0.32	18
B band	6A	$(2.28 \pm 0.42) \times s_{(B)}^{-1} - (21.49 \pm 0.41)$	0.17	21
	6B	$(1.08 \pm 0.24) \times s_{(B)}^{-1} - (20.30 \pm 0.24)$	0.23	46
V band	6A	$(2.58 \pm 0.38) \times s_{(B)}^{-1} - (21.67 \pm 0.38)$	0.20	21
	6B	$(1.10 \pm 0.24) \times s_{(B)}^{-1} - (20.22 \pm 0.25)$	0.22	46
R band	6A	$(1.88 \pm 0.57) \times s_{(B)}^{-1} - (20.96 \pm 0.56)$	0.18	14
	6B	$(0.75 \pm 0.29) \times s_{(B)}^{-1} - (19.89 \pm 0.30)$	0.26	34
I band	6A	$(1.10 \pm 0.61) \times s_{(B)}^{-1} - (19.93 \pm 0.60)$	0.23	20
	6B	$(0.52 \pm 0.30) \times s_{(B)}^{-1} - (19.41 \pm 0.31)$	0.27	42

6A is 'BV bluest' sample.
6B is 'BV bluest' + 'BV bluer' sample.

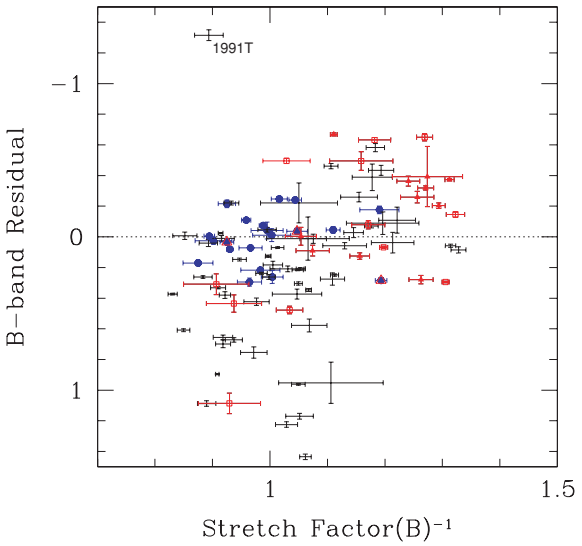

Figure 19. Residuals from the stretch–magnitude relation derived from 'BV bluest' SNe Ia without dust/colour correction. Filled blue circles are 'BV bluest' SNe Ia (sample 7A in Table 7), red symbols are SNe Ia hosted by E or S0 galaxies (sample 7B in Table 7), filled red triangles are 'BV bluer' SNe Ia hosted by E or S0 galaxies (sample 7C in Table 7), open red triangles with filled blue circle are 'BV bluest' SNe Ia hosted by E or S0 galaxies (sample 7D in Table 7) and the other symbols are for other SNe Ia.

Table 7. rms of the stretch–magnitude relation of the samples and their average $(B-V)_{\max}$.

Sample	rms (mag)	Average $(B-V)_{\max}$	Number
7A	0.17	−0.12	21
7B	0.51	0.04	27
7C	0.30	−0.07	15
7D	0.17	−0.12	3

7A is 'BV bluest' sample.
7B is sample hosted by E or S0 galaxies with no colour selection.
7C is 'BV bluer' sample hosted by E or S0 galaxies.
7D is 'BV bluest' sample hosted by E or S0 galaxies.

6.1 Colour correction for absolute magnitude

It is known empirically that correcting the luminosity of SNe Ia based on their colours will decrease the dispersion of peak B-band luminosities. For example, MLCS, CMAGIC and SALT use colour information as part of the light-curve fitting technique, while the Stretch and Δm_{15} methods use colour information to decrease the dispersion after fitting light curves. We also introduce colour terms to decrease the dispersion around the stretch–magnitude relation.

We need a colour excess to remove the extinction due to dust in the host galaxy, and the intrinsic colour of each SN Ia to correct for diversity among SNe Ia. However, it is difficult to separate an observed colour excess into the intrinsic colour of the SN and the reddening by dust. Therefore, we do not try to distinguish them; instead, we use the observed colour of SNe Ia empirically to reduce the dispersion of the relationship between absolute magnitude and inverse stretch factor. We employ a χ^2-fitting technique with following equation:

$$\chi = M_B - [a \times s_{(B)}^{-1} + b \times (B-V)_{\max} + c]. \quad (3)$$

Here, M_B is the absolute B-band magnitude at maximum shown in Table 2 without any corrections, $(B-V)_{\max}$ is the apparent colour at B-band maximum and a, b and c are fitting parameters. Note that here we treat $(B-V)_{\max}$ as independent from the B-band stretch factor.

Table 8 shows the inverse B-band stretch factor and B-band luminosity relationships, including the rms of each sample. The rms is the smallest in sample 8D, which includes SNe Ia hosted by E or S0 galaxies at higher redshift ($z > 0.02$). The relationship of sample 8D is similar to that of sample 8B (SNe at $z > 0.02$), but the rms is smaller in the sample drawn from E or S0 galaxies. This may indicate that extinction by dust in an E or S0 host galaxy is smaller than extinction in other types of galaxies, if both sample 8B and 8D have the same intrinsic dispersion of peak B-band luminosity.

7 HOST GALAXY DUST PROPERTIES

There are several approaches to estimate the effects of extinction by dust in host galaxies. In this section, we estimate host galaxy dust extinction using the apparent colours of SNe Ia. Dust in a host galaxy makes the apparent colour of a SN Ia redder, so we can estimate how a host galaxy obscures a SN using colour information. We use the following relationship:

$$A_X = R_X \times E(M_B - M_V). \quad (4)$$

Here, A_X is dust absorption in the X band, R_X is the ratio of total to selective extinction in the X band and $E(M_B - M_V)$ is the colour excess. We derive $E(M_B - M_V)$ assuming an intrinsic $(B-V)_{\max}$ colour for each SN Ia and extract the excess from observed colour.

There are two main problems when we use equation (4) to correct for extinction in the host galaxy. One problem is that we do not know if the properties of dust in host galaxies are the same as those of dust in the Milky Way, especially the value of R_X. ALT04 and other works showed that R_B of dust in host galaxies may be smaller than R_B of dust in the Milky Way. Another problem is that we do not

Table 8. Relationships between B-band inverse stretch factor and luminosity with colour term and rms of the stretch–magnitude relation.

Sample	Relation	rms (mag)	Number
8A	$(0.96 \pm 0.28) \times s_{(B)}^{-1} - (2.51 \pm 0.15) \times (B-V)_{\max} - (20.26 \pm 0.29)$	0.48	108
8B	$(0.98 \pm 0.18) \times s_{(B)}^{-1} - (2.28 \pm 0.28) \times (B-V)_{\max} - (19.95 \pm 0.19)$	0.27	50
8C	$(1.09 \pm 0.59) \times s_{(B)}^{-1} - (1.78 \pm 0.43) \times (B-V)_{\max} - (20.15 \pm 0.71)$	0.33	27
8D	$(0.99 \pm 0.34) \times s_{(B)}^{-1} - (2.23 \pm 0.24) \times (B-V)_{\max} - (20.10 \pm 0.41)$	0.12	15

8A is all SNe Ia.
8B is SNe Ia of $z > 0.02$.
8C is SNe Ia hosted by E or S0 galaxies.
8D is SNe Ia of $z > 0.02$ hosted by E or S0 galaxies.

Table 9. Dispersion of B-band luminosities (mag) of selected redder SNe Ia after host galaxy dust correction based on three different conversion factors of R_B.

Sample	$R_B = 4.315$	$R_B = 3.5$	$R_B = 3.0$	Number
All	0.89	0.81	0.79	53
9A	0.99	0.90	0.89	38
9B	0.56	0.48	0.45	15
ALT04	0.52	0.44	0.42	55

9A is 'broader' LC sample, for which $s_{(B)}^{-1} < 1.1$.
9B is 'narrower' LC sample, for which $s_{(B)}^{-1} > 1.1$.
ALT04 is common 55 samples with ALT04, Fig. 5(b).

know the intrinsic colour of SNe Ia. Usually, we assume that the bluest SNe Ia are free from extinction, but there is no guarantee that all SNe Ia have the same intrinsic colour as the bluest examples. These two problems make the correction difficult. Hence, we reduce the problem to two extreme cases in the following.

In case A, we assume that the intrinsic colour of SNe Ia depends on the inverse B-band stretch factor. This assumption was also used in ALT04. We found earlier that the intrinsic $(B-V)_{\max} = -0.30 \times s_{(B)}^{-1} + 0.18$ from the relations between $s_{(B)}^{-1}$ and B, V band (see Table 6). This assumption is consistent with SNe Ia with $s_{(B)}^{-1} < 1.1$, but not consistent with SNe Ia with $s_{(B)}^{-1} > 1.1$ (see Fig. 15).

In case B, we assume the intrinsic colour of SNe Ia is constant, and has some significant scatter. In this case, even if two SNe Ia have the same inverse B-band stretch factor, they do not necessarily have the same colour.

First, we tried to correct for extinction due to dust in host galaxies under the assumption of case A, using three different values for R_B: 4.315 (appropriate for the Milky Way, Schlegel et al. 1998), 3.5 (ALT04) and 3.0. We selected redder SNe Ia, which are $(B-V)_{\max} > -0.02$ (0.1 mag redder from average 'intrinsic' $(B-V)_{\max} = -0.12$ derived from Fig. 9). These SNe Ia must be significantly reddened by dust in the host galaxy. Table 9 shows the scatter around the stretch–magnitude relationship in B-band luminosity after we have corrected for extinction according to equation (4). Though smaller values of R_B do decrease the dispersion, the scatter is still large. This means we must introduce another factor to account for the large dispersion; for example, some intrinsic scatter of $(B-V)_{\max}$. Note that the rms of all samples after our corrections for dust in the host galaxy is larger than the rms shown in ALT04, Fig. 5(b) ($R_B = 3.5$, $\sigma = 0.31$). The explanation is mainly that we used only redder SNe in our analysis, but the ALT04 sample includes bluer SNe Ia which have smaller scatter in B-band luminosity than redder SN Ia. If we use a set of 55 SNe Ia in common with ALT04 to derive the dispersion, we find $\sigma = 0.44$ mag with $R_B = 0.35$, which is smaller than that of redder SN Ia ($R_B = 3.5$, $\sigma = 0.81$, Table 9) but still larger than the result shown in ALT04, Fig. 5(b) ($R_B = 3.5$, $\sigma = 0.31$). The reason may be in the details of how one derives $E(B-V)$: ALT04 used a weighted average of $(B-V)_{\max}$ and $(B-V)_{\rm tail}$, but we used $(B-V)_{\max}$ only.

Next, we tried to correct host galaxy dust extinction under the assumption of case B (a constant intrinsic colour for all SNe Ia) using a factor $R_B = 4.315$. Indeed, according to Fig. 11, there is no basis to assume that dust in host galaxies has properties different from dust in the Milky Way. Under the assumption of case B, we cannot derive A_X from equation (4) because we do not know the intrinsic $(B-V)_{\max}$ of SNe Ia. Instead, we tried to derive $E(M_B - M_V)$ from the following equation (5), under the assumption that the intrinsic B-band luminosity of SNe Ia is given by the relationships listed in Table 6.

$$E(M_B - M_V) = \frac{M_B - (2.28 \times s_{(B)}^{-1} - 21.49)}{R_{\rm MW}}. \quad (5)$$

Here, we regard residuals from the intrinsic B-band luminosity at some particular B-band stretch factor as due completely to extinction by dust in the host galaxy, and we divide the residuals by $R_{\rm MW} = 4.315$, the ratio of total to selective extinction for dust in the Milky Way. We applied equation (5) to dust-affected SNe Ia, corrected them for reddening, then compared their $(B-V)_{\max}$ distribution with that of dust-free SNe Ia.

To make the dust-affected sample, we selected SNe Ia which are fainter by at least 1.0 mag in B-band than the intrinsic luminosity derived from inverse B-band stretch factor. For the dust-free sample, we selected SNe Ia which fall within 0.17 mag (which is one standard deviation of 'BV bluest' SNe Ia) of the relationship between intrinsic luminosity and inverse B-band stretch factor.

The results are distributions of $(B-V)_{\max}$ colours for dust-free samples, dust-affected samples and dust-corrected samples, using B-band residuals to correct for extinction (Fig. 20) or V-band residuals to correct for extinction (Fig. 21). We compare the distribution of SNe Ia which are corrected using the factor R_B of the Milky Way to the distribution of SNe Ia which are corrected with a smaller factor R_B. These comparisons show that if we accept the idea that intrinsic SNe Ia colours have an intrinsic dispersion which is similar to that of the 'reference' samples in Figs 20 and 21, the average factor R of dust in host galaxies is not different than that for dust in the Milky Way. We ran a Kolmogorov–Smirnov test on the distribution of corrected $(B-V)$ colours and found no significant difference between them. Intrinsic diversity among SNe Ia has also been shown by previous spectroscopic studies. Berian et al. (2006), for example, showed that rms of B- and V-band

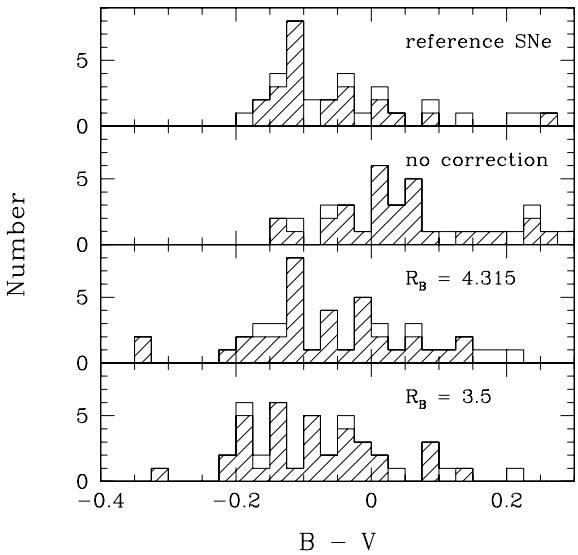

Figure 20. Distributions of $(B-V)_{\max}$ of dust-free and dust-corrected SNe Ia using B-band brightness. The top panel is reference SNe Ia which are mostly dust-free. The second panel is for SNe Ia which are significantly affected by host galaxy dust, but without dust corrections. The third panel is after dust correction using $R_B = 4.315$ (Schlegel et al. 1998), and the bottom panel is dust correction with $R_B = 3.5$ (ALT04). Shaded bars show SNe Ia with broader light-curve shape, $s_{(B)}^{-1} < 1.1$, which are expected to be spectroscopically 'normal' SNe Ia (see Fig. 14).

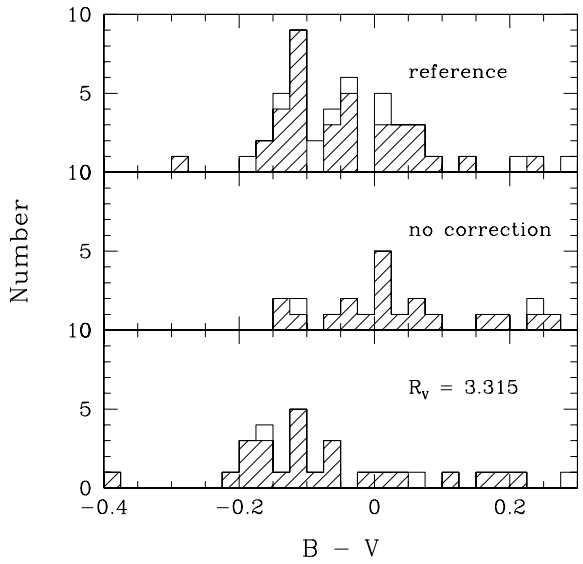

Figure 21. Distribution of $(B-V)_{\rm max}$ of dust-free and dust-corrected SNe Ia using V-band brightness. The top panel is reference SNe Ia which are mostly dust-free. The middle panel is for SNe Ia which are significantly affected by dust, but without dust corrections. The bottom panel is after dust correction with $R_V = 3.315$ (Schlegel et al. 1998). Shaded bars show SNe Ia with broader light-curve shape, $s_{(B)}^{-1} < 1.1$, which are expected to be spectroscopically 'normal' SNe Ia (see Fig. 14).

luminosities is about 0.1–0.2 mag, and their results are consistent with ours.

If the intrinsic colours of SNe Ia have a significantly large scatter, it is very difficult to correct properly for extinction by dust in host galaxies with photometric measurements only.

8 SN IA SAMPLES FOR COSMOLOGY

In Section 6, we studied the connection between light-curve shape and luminosity and looked for ways to decrease the dispersion around the relationship. In Section 7, we checked the properties of dust in host galaxies.

These results suggest that if one wishes to use SN Ia as standard candles, one should take one of the following approaches. First, one might select only 'BV bluest' SNe Ia. As we showed in Section 6.1, colour corrections make the dispersion smaller, but the improvement in the dispersion of a combined sample of 'BV bluer' and 'BV bluest' SNe Ia after colour corrections is only 0.02 mag, and their rms is still larger than that of the 'BV bluest' sample with no colour correction. In addition, Fig. 15 shows that the intrinsic colour of SNe Ia seems to have a large scatter, and that even SNe which have same B-band stretch factor may not have same intrinsic colour. Until we solve two puzzles: (i) how to separate the apparent colour of SNe Ia into intrinsic colour and reddening due to the host galaxy and (ii) the value of the ratio of total to selective extinction R and its evolution from the low- to the high-z Universe, we had better not use colour corrections in samples which have large colour diversity. The study of K-corrections is very important for selecting 'BV bluest' SN Ia and determining extinction by dust in host galaxies.

Another approach is to select SNe Ia which occur in E or S0 galaxies. As shown in Section 6.1, the rms of stretch–magnitude relationship of colour-corrected SNe Ia hosted by distant E or S0 galaxies (8D, Table 8) is 0.12 mag, which is smaller than that of the 'BV bluest' SNe Ia discussed above. However, the properties of SNe Ia in E or S0 galaxies tend to differ from those of SNe Ia within other types of galaxies (cf. Figs 14, 19 and 15). This means we may have to apply different relations to SNe Ia hosted by E or S0 galaxies.

Even if we select SNe Ia within early-type galaxies, those SNe are not always free from dust, as shown in Fig. 11. This is consistent with the idea that not only interstellar dust but also dust surrounding the SN affects the light from SNe Ia, as Wang (2005) pointed out. Patat et al. (2007) reported the spectroscopic detection of circumstellar dust around normal SNe Ia. The SNe Ia occurring in early-type galaxies also tend to have narrower light-curve widths, with inverse B-band stretch factor >1.1 (see Fig. 15), and they have larger intrinsic dispersion in SED as shown in Fig. 15. Fig. 19 shows that these SNe Ia in early-type galaxies have larger dispersion than 'BV bluest' SNe Ia or that the stretch–magnitude relation is different from that of 'BV bluest' SNe Ia. Our results are consistent with the distribution of B-band stretch factors of nearby SNe Ia within E or S0 hosts determined in Sullivan et al. (2006). However, Sullivan et al. (2003) also claimed that at high redshifts, the scatter in luminosity of SNe Ia hosted by E or S0 galaxies is smaller than that of SNe Ia inside spiral galaxies.

In any case, we must know whether or not the properties of SNe Ia in the low-z Universe and the high-z Universe are the same, since it is important when we apply stretch–brightness relationships or make K-corrections. To answer these questions, we need to study the nature of SNe Ia at all redshifts.

9 SUMMARY

In this work, we re-analyse U-, B-, V-, R- and I-band light curves of 122 previously published nearby (redshift <0.11) SNe Ia, which are mainly from JHA06, Riess et al. (1999a) and Hamuy et al. (1996a). We devise the 'Multiband Stretch method', which is a revised Stretch method extended to fitting up to five bands. We create new U-, B-, V-, R- and I-band light-curve templates from well-observed SNe Ia for our 'Multiband Stretch method'. It is known that the I-band light curves of SNe Ia show much variation. However, we found our I-band template fitted about 90 per cent of SNe Ia I-band light curves very well.

Using the results of our light-curve fitting, we examine the relationships between luminosity, colours at maximum light and stretch factors. In Section 5, we show a possible subgroup of SNe Ia which have different colours from the main group of SNe Ia; this subgroup tends to be found in E or S0 galaxies. In Section 6, we find the relationship between inverse B-band stretch factor and U-, B-, V-, R- and I-band luminosity, using colour-selected SNe Ia to avoid contamination from the outlying subgroup. We obtain a stretch–magnitude relationship for 'BV bluest' SNe Ia without colour correction as $(2.28 \pm 0.42) \times s_{(B)}^{-1} - (21.49 \pm 0.41)$, which is steeper than the slope of the corresponding stretch–magnitude relation in ALT04. The rms of the residuals from this relationship is 0.17 mag. If we attempt to reduce the dispersion in luminosity by using colour corrections, we find that for distant (redshift >0.02) SNe Ia, $M_B = 0.98 \times s_{(B)}^{-1} - 2.28 \times (B-V)_{\rm max} - 19.95$ with an rms of 0.27 mag. The rms becomes 0.12 mag when we select only SNe Ia hosted by E or S0 galaxies. In Section 7, we statistically investigate the properties of dust in host galaxies, and find that the ratio of total to selective extinction R can be consistent with that of dust in the Milky Way if we assume that SNe Ia have some diversity in their intrinsic colours.

Based on these results, in Section 8, we discuss how to select subsets of SNe Ia which may be good distance indicators for

cosmology. We find two possibilities: one is to use only 'BV bluest' SNe Ia with broad light curves, and the other is to use only SNe Ia inside E or S0 galaxies. To use these samples for precision cosmology, we need to study the properties of SNe Ia from the low- to the high-z Universe.

ACKNOWLEDGMENTS

We are grateful to all the people who observed and analysed the SNe Ia used in this paper. We are also grateful to members of the SDSS-II Supernova Survey and Supernova Cosmology Project for useful discussions. We thank Saul Perlmutter and David Rubin for discussion and comments on SNe Ia hosted by elliptical galaxies. We also thank Michael Richmond for carefully reading the manuscript. This work is supported in part by a JSPS core-to-core programme 'International Research Network for Dark Energy' and by a JSPS research grant (17104002).

REFERENCES

Aldering G. et al., 2002, SPIE, 4836, 61
Aldering G. et al., 2006, ApJ, 650, 510
Altavilla G. et al., 2004, MNRAS, 349, 1344 (ALT04)
Anupama G. C., Sahu D. K., Jose J., 2005, A&A, 429, 667
Astier P. et al., 2006, A&A, 447, 31
Benetti S. et al., 2005, AJ, 623, 1011
Berian J. J. et al., 2006, MNRAS, 370, 933
Bessell M. S., 1990, PASP, 102, 1181
Branch D., Tammann G. A., 1992, A&A, 30, 359
Branch D., Fisher A., Nugent P., 1993, AJ, 106, 2383
Contardo G., Leibundgut B., Vacca W. D., 2000, A&A, 359, 876
Deng J., Kawabata K. S., Ohyama Y., 2004, ApJ, 605, L37
Ford C. H., Herbst W., Richmond M. W., Baker M. L., Filippenko A. V., Treffers R. R., Paik Y., Benson P. J., 1993, AJ, 106, 1101
Frieman J. et al., 2008, AJ, 135, 338
Garnavich P. M. et al., 2004, ApJ, 613, 1120
Germany L. M., Reiss D. J., Schmidt B. P., Stubbs C. W., Suntzeff N. B., 2004, A&A, 415, 863
Goldhaber G. et al., 2001, ApJ, 558, 359
Guy J., Astier P., Nobili S., Regnault N., Pain R., 2005, A&A, 443, 781
Guy J. et al., 2007, A&A, 466, 11
Hamuy M., Phillips M. M., Wells L. A., Maza J., 1993, PASP, 105, 787
Hamuy M. et al., 1996a, AJ, 112, 2408
Hamuy M., Phillips M. M., Suntzeff N. B., Schommer R. A., Maza J., Aviles R., 1996b, AJ, 112, 2391
Ho W. C. G., Van D. S. D., Peng C. Y., Filippenko A. V., Leonard D. C., Matheson T., Treffers R. R., Richmond M. W., 2001, PASP, 113, 1349
Howell D. A., 2001, ApJ, 554, L193
Howell D. A. et al., 2006, Nat, 443, 308
Jha S. et al., 2006, AJ, 131, 527 (JHA06)
Jha S., Riess A. G., Kirshner R. P., 2007, ApJ, 659, 122
Kim A., Goobar A., Perlmutter S., 1996, PASP, 108, 190
Knop R. A. et al., 2003, ApJ, 598, 102
Krisciunas K., Hastings N. C., Loomis K., McMillan R., Rest A., Riess A. G., Stubbs C., 2000, ApJ, 539, 658
Krisciunas K. et al., 2001, AJ, 122, 1616
Krisciunas K. et al., 2003, AJ, 125, 166
Krisciunas K. et al., 2004a, AJ, 127, 1664
Krisciunas K. et al., 2004b, AJ, 128, 3034
Kuntal M., Atish P. K., Bhattacharya D., 2005, MNRAS, 360, 662
Li W. et al., 2001, PASP, 113, 1178
Li W. et al., 2003, PASP, 115, 453
Lira P. et al., 1998, AJ, 115, 234
Mannucci F., Della V. M., Panagia N., Cappellaro E., Cresci G., Maiolino R., Petrosian A., Turatto M., 2005, A&A, 433, 807
Modjaz M., Li W., Filippenko A. V., 2001, PASP, 113, 308
Nobili S. et al., 2005, A&A, 437, 789
Nugent P., Kim A., Perlmutter S., 2002, PASP, 114, 803
Patat F., Benetti S., Cappellaro E., 1996, MNRAS, 278, 111
Patat F. et al., 2007, Sci, 317, 924
Perlmutter S. et al., 1997, in Ruiz-Lapuente P., Canal R., Isern J., eds, Thermonuclear Supernova. Dordrecht, Kluwer, p. 749
Perlmutter S. et al., 2005, ApJ, 517, 565
Phillips M. M., 1993, ApJ, 413, 105L
Phillips M. M., Lira P., Suntzeff N. B., Schommer R. A., Hamuy M., Maza J., 1999, AJ, 118, 1766
Pignata G. et al., 2004, MNRAS, 355, 178
Prieto J. L., Armin R., Suntzeff N. B., 2006, ApJ, 647, 501
Pritchet C. J. and The SNLS Collaboration, 2005, in Wolff S. C., Lauer T. R., eds, ASP Conf. Ser. Vol. 339, Observing Dark Energy. Astron. Soc. Pac., San Francisco, p 60
Quimby R., Hoflich P., Wheeler J. C., 2007, ApJ, 666, 1083
Reindl B., Tammann G. A., Sandage A., Saha A., 2005, ApJ, 624, 532
Richmond M. W. et al., 1995, AJ, 109, 2121
Riess A. G., Press W. H., Kirshner R. P., 1996, ApJ, 473, 88
Riess A. G. et al., 1998, AJ, 116, 1009
Riess A. G. et al., 1999a, AJ, 117, 707
Riess A. G., Filippenko A. V., Li W., Schmidt B. P., 1999b, AJ, 118, 2668
Riess A. G. et al., 2004, ApJ, 607, 665
Riess A. G. et al., 2005, ApJ, 627, 579
Sahu D. K., Anupama G. C., Prabhu T. P., 2006, MNRAS, 366, 682
Sako M. et al., 2008, AJ, 135, 348
Schlegel D. J., Finkbeiner D. P., Davis M., 1998, ApJ, 500, 525
Spergel D. N. et al., 2007, ApJS, 170, 377
Strolger L. G. et al., 2002, AJ, 124, 2905
Sullivan M. et al., 2003, MNRAS, 340, 1057
Sullivan M. et al., 2006, ApJ, 648, 868
Suntzeff N. B. et al., 1999, AJ, 117, 1175
Valentini G. et al., 2003, ApJ, 595, 779
van den Bergh S., Li W., Filippenko A. V., 2005, PASP, 117, 773
Vinko J. et al., 2003, A&A, 397, 115
Wang L., 2005, AJ, 635, L33
Wang L., Goldhaber G., Aldering G., 2003, ApJ, 590, 944
Wells L. A. et al., 1994, AJ, 108, 2233
Wood-Vasey W. M. et al., 2007, ApJ, 666, 694

This paper has been typeset from a TEX/LATEX file prepared by the author.